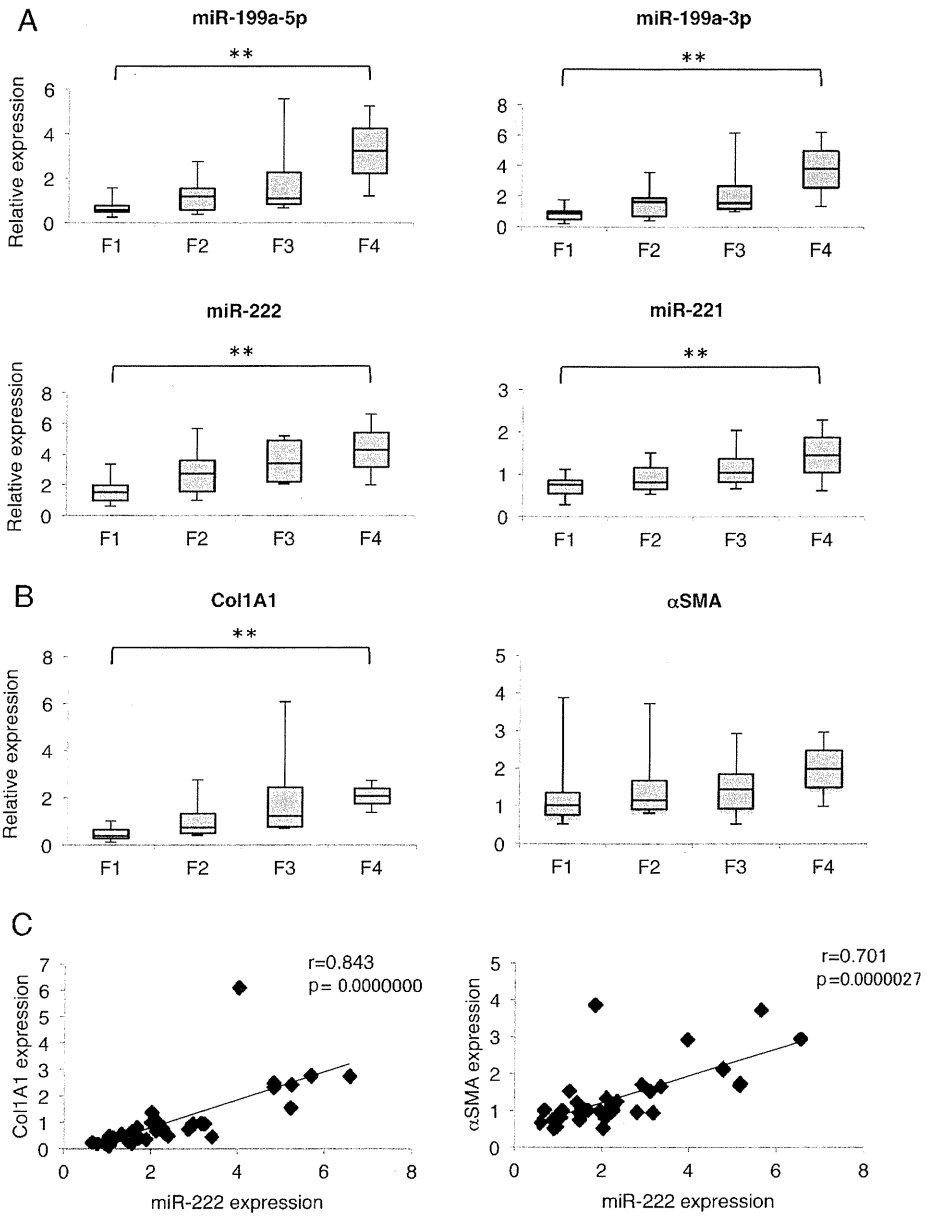

Figure 2 MicroRNA (miRNA) levels and their correlations with Col1A1 and α-smooth muscle actin (αSMA) mRNA expression in patients with chronic hepatitis C. (A) Expression of miR-199a-5p, miR-199a-3p, miR-222 and miR-221 in 35 patients with hepatitis C virus (HCV) with fibrosis. The expression levels are indicated relative to F1. The Jonckheere–Terpstra test for ordered alternatives was used to identify trends among classes. **p<0.01. (B) Expression of Col1A1 and αSMA mRNAs in 35 patients with HCV with fibrosis. The expression levels are indicated relative to F1. Glyceraldehyde 3-phosphate dehydrogenase was used as an internal control. The Jonckheere–Terpstra test for ordered alternatives was used to identify trends among classes. **p<0.01. (C) Correlation between miR-222 expression and Col1A1 or αSMA mRNA expression. Correlation coefficients between parameters were evaluated by Spearman rank correlations.

area. These mouse livers exhibited significant upregulation of the expression of Col1A1 (3.1-fold, p<0.05) and αSMA (1.9-fold, p<0.05) mRNAs compared with the control livers at 8 weeks (figure 4B). The expression of miR-221 and miR-222 increased by 1.8-fold (p=0.06) and 1.4-fold (p<0.01), respectively, at 8 weeks after TAA injection (figure 4C). The increased expression of miR-222 was accompanied by increased Col1A1 (p<0.05) and αSMA mRNA expression (p<0.01) (data not shown). Another liver fibrosis model was produced in mice by feeding them an MCDD. miR-221 and miR-222 increased by 2.4-fold (p<0.01) and 2.6-fold (p<0.01), respectively, in livers of mice fed MCDD for 15 weeks compared with those fed MCCD for 15 weeks (figure 4D). These results confirm that the increased expression of miR-221/222 in fibrotic livers is reproduced in mouse models. In addition, miR-221 and miR-222 expression increased in rats administered MCDD for 10 weeks, but returned to the level of the controls after 2 weeks on MCCD in the recovery group (figure 4E). These data clearly indicate the correlation between the increase in miR-221/222 and liver fibrosis.

Expression of miR-222 in hepatic stellate cells

According to the data obtained from human and rodent fibrotic livers, we assumed that stellate cells may contribute to the increases of miR-222 and its homologue miR-221. As expected, the expression of both miR-221 and miR-222 increased during the activation process of mouse stellate cells in primary culture (6.1- and 26.8-fold increases in miR-221 and 4.1- and 13.9-fold increases in miR-222 at day 4 and day 7 compared with day 1, respectively), in a manner similar to the mRNA expression of Col1A1 and αSMA (38.3- and 61.3-fold increases in Col1A1 mRNA and 6.1- and 6.9-fold increases in αSMA at day 4 and day 7 compared with day 1, respectively) (figure 5A,B). Isolated mouse hepatocytes expressed both miRNAs in smaller amounts than with the activated stellate cells (figure 5A). In addition, both miR-221 and miR-222 expression were significantly higher in LX-2 than in HepG2 cells (9.5- and 6.0-fold, respectively), Huh7 cells (9.2- and 4.4-fold, respectively) and NIH3T3 cells (1.1- and 3.2-fold, respectively) (figure 5C), confirming the relative specificity of the miRNA expression in activated stellate cells.

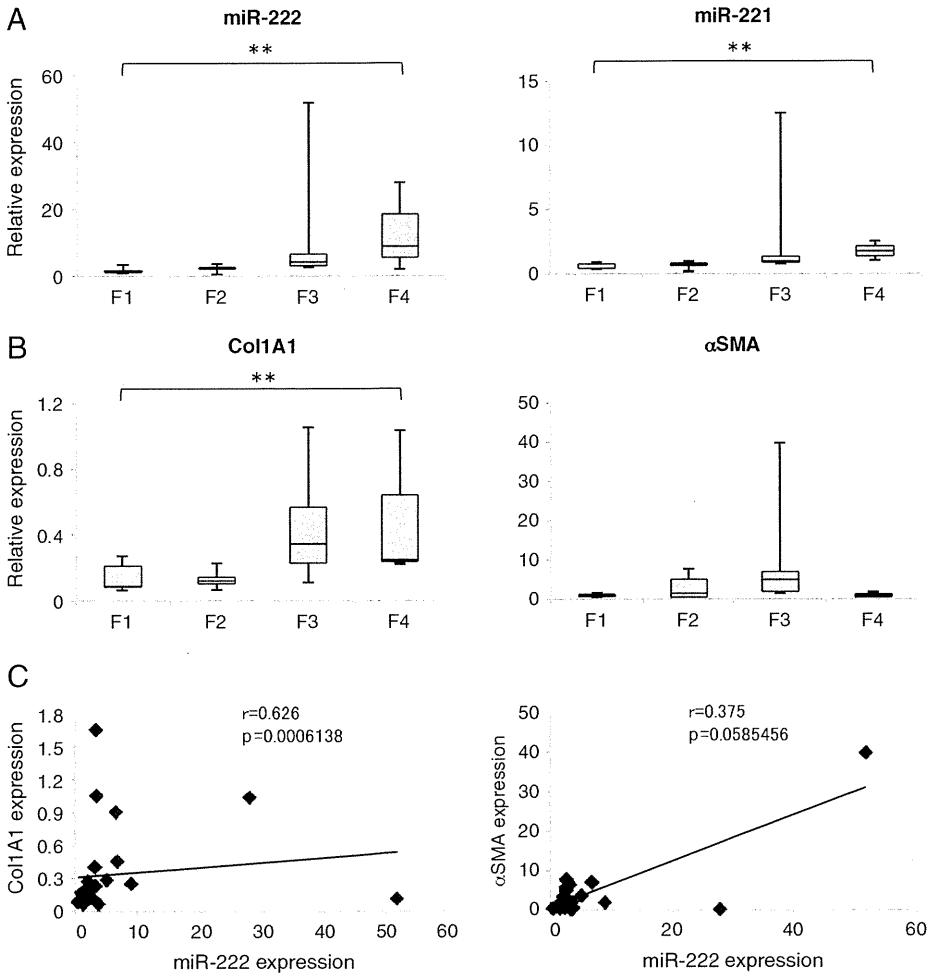

Figure 3 Levels of microRNA (miRNA)-221/222 and their correlation with Col1A1 and α-smooth muscle actin (αSMA) mRNA levels in patients with non-alcoholic steatohepatitis (NASH). (A) Expression of miR-221/222 in 26 patients with NASH. The expression levels are indicated relative to F1. The Jonckheere–Terpstra test for ordered alternatives was used to identify trends among classes. **p<0.01. (B) Expression of Col1A1 and αSMA mRNAs in 26 patients with NASH. The expression levels are indicated relative to F1. Glyceraldehyde 3-phosphate dehydrogenase was used as an internal control. The Jonckheere–Terpstra test for ordered alternatives was used to identify trends among classes. **p<0.01. (C) Correlation between miR-222 expression and Col1A1 or αSMA mRNA expression. Correlation coefficients between parameters were evaluated by Spearman rank correlations.

miR-222 transcription is regulated by NF-κB; the genomic region upstream of human miR-222 has multiple NF-κB binding elements.[33] NF-κB regulates Col1A1 gene expression and stellate cell activation.[34–36] Thus, we studied whether NF-κB stimulators, such as TGFα and TNFα, induce miR-222 expression and, in contrast, whether an NF-κB inhibitor (QNZ) inhibits its expression. As shown in figure 5D, stimulation of stellate cells with TGFα (1 or 10 ng/ml) or TNFα (0.1 or 1 ng/ml) for 24 h from day 1 to day 2 upregulated miR-222 expression, while QNZ (10 or 100 nmol/l) significantly reduced it. Stimulation of stellate cells with TGFα (1 ng/ml) or TNFα (0.1 ng/ml) for 72 h from day 1 to day 4 upregulated miR-222 expression by 1.9-fold (p<0.01) or 1.3-fold (p<0.05), respectively, compared with the untreated control (figure 5E) and miR-222 upregulation was inhibited to 18% or 26% of the untreated control level, respectively, by QNZ (figure 5E). These results indicate that miR-222 expression in stellate cells is regulated by NF-κB activation. QNZ (10 nmol/l) inhibited the activation-associated morphological transition of mouse hepatic stellate cells (figure 5F). This condition attenuated the expression of Col1A1 mRNA to 21% (p<0.01) and αSMA mRNA to 63% (p<0.01) of the untreated control levels (figure 5G).

Interaction of miR-222 with the *CDKN1B* 3′UTR in human stellate cells

miR-221 controls CDKN1B and CDKN1C expression in HCC cell lines.[37] The prediction of miRNA target regions by TargetScan (http://www.targetscan.org/) indicated that the *CDKN1B* 3′UTR has two target regions for miR-221/222 (figure 6A). Here, we investigated the presence of a direct interaction between miR-222 and CDKN1B mRNA in LX-2 cells by the firefly luciferase reporter assay and found that the miR-222 precursors inhibited luciferase activity derived from vectors carrying the *CDKN1B* 3′UTR (figure 6B). These observations indicate that the *CDKN1B* 3′UTR could be targeted by miR-222 in LX-2 cells.

Next, we transfected miR-222 precursors and miR-222 inhibitors into LX-2 cells. The transient transfection of miR-222 precursors significantly inhibited CDKN1B mRNA and protein expression compared with their expression in cells transfected with the negative control miRNA (figure 6C). Additionally, the transfection of miR-222 inhibitors significantly upregulated CDKN1B mRNA and protein expression in comparison with cells transfected with the negative control miRNA (figure 6D). Even though the transfection of miR-222 precursors or inhibitors into LX-2 cells showed negligible effects on cell growth (figure 6E,F), these results indicate that miR-222 targets *CDKN1B* in LX-2 cells.

Additional analyses indicated that transient transfection with miR-222 precursors significantly upregulated Col1A1 and matrix metalloproteinase 2 (MMP-2) mRNA expression and downregulated MMP-1, MMP-9 and TGFβ1 mRNA expression via unknown mechanisms (figure 6G).

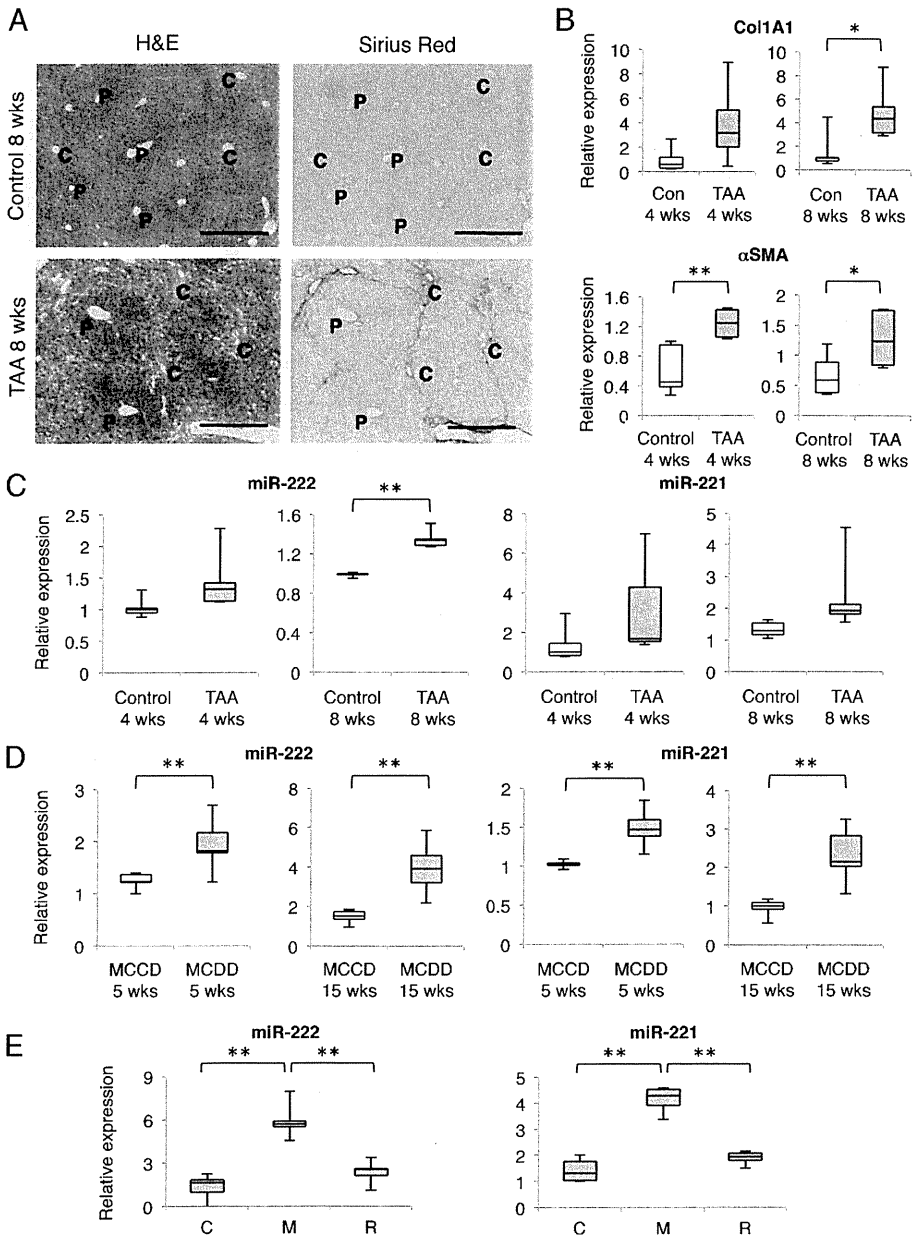

Figure 4 Expression of miR-221/222 in mouse models of liver fibrosis. (A) Liver fibrosis was induced in mice by injecting 200 μg/g body weight of thioacetamide (TAA) for 8 weeks. Haematoxylin and eosin staining (H&E; left). Sirius red staining (right). Scale bars, 200 μm. C, central vein area; P, portal vein area. (B) mRNA expression of Col1A1 and α-smooth muscle actin (αSMA) in TAA-induced liver fibrosis. The expression levels are indicated relative to control livers. Glyceraldehyde 3-phosphate dehydrogenase was used as an internal control. *p<0.05, **p<0.01 compared with control. (C) Expression of miR-221 and miR-222 in TAA-induced liver fibrosis. The expression levels are indicated relative to control livers. **p<0.01 compared with control. In B and C, open columns indicate data from controls and closed columns from TAA. (D) Expression of miR-221 and miR-222 in a methionine- and choline-deficient diet (MCDD)-induced liver fibrosis. The expression levels are indicated relative to methionine-choline control diet (MCCD) mouse livers. **p<0.01 compared with MCCD. Open columns indicate data from MCCD and closed columns from MCDD. (E) Expression of miR-221 and miR-222 in MCDD-induced liver fibrosis in rats.[27] The expression levels are indicated relative to rats fed MCCD for 10 weeks (C). Liver miR-221 and miR-222 levels significantly decreased in the recovery phase (R, MCDD for 8 weeks followed by MCCD for 2 weeks) compared with those fed MCDD for 10 weeks (M). **p<0.01.

DISCUSSION

Our study explored miRNA expression profiles during the progression of liver fibrosis in patients infected with HCV using microarray analysis. The expression of miR-222 was significantly correlated with that of Col1A1 and αSMA mRNAs in patients with HCV and with the expression of miR-221. To our knowledge, this is the first report to identify miR-221 and miR-221 as fibrosis-related molecules and to report miR-221/222 expression in a liver pathology other than carcinogenesis. Our results additionally indicate the close correlation between miR-221/222 and Col1A1 mRNA expression in the livers of people with NASH.

Recently, Roderburg *et al* reported the upregulation of miR-125-5p, miR-199b-3p, miR-221 and miR-302 and the downregulation of miR-29 family members in CCl_4-treated mouse livers, as observed using microarray analysis and quantitative RT-PCR.[38] Murakami *et al* reported that increased miR-199a-5p, miR-199a-3p, miR-200a and miR-200b levels are significantly associated with the progression of liver fibrosis in both humans and mice and that the overexpression of miR-199a-3p in human stellate cells results in the significant induction of tissue inhibitor of MMP-1, Col1A1 and MMP-13.[32] Furthermore, the expression levels of miR-21 and miR-122 have been correlated with the histological findings of HCV-induced liver disease.[23] However, in our analyses, although the expression of miR-199a-5p, miR-199a-3p and miR-21 tended to increase in activated mouse stellate cells during culture (0.8- and 2.1-fold for miR-199a-5p, 0.7- and 1.5-fold for miR-199a-3p and 1.9- and 3.8-fold for miR-21 at day 4 and day 7, respectively, compared with day 1), they failed to increase more than 10-fold, as miR-221 and miR-222 did (data not shown). Thus, miR-222 and miR-221 are more likely to reflect the activation of stellate cells than miR-199a-5p, miR-199a-3p and miR-21, similarly to the expression of Col1A1 mRNA.

It is generally accepted that liver fibrosis is a major risk factor for the development of HCC. A national surveillance

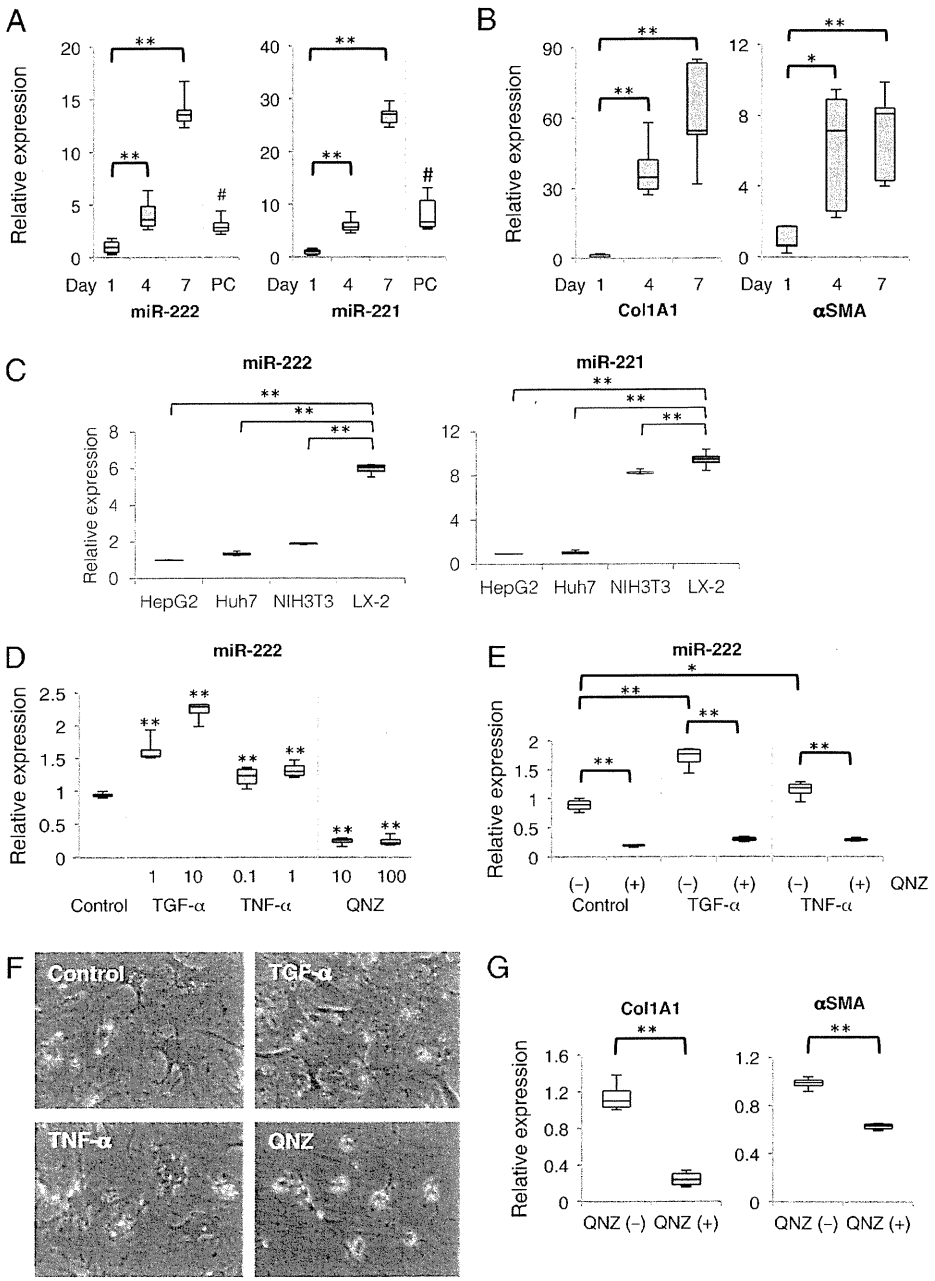

Figure 5 Regulation of miR-222 expression in stellate cells. (A) Expression of miR-221 and miR-222 in mouse stellate cells during primary culture. Isolated mouse stellate cells were cultured for the indicated periods. **p<0.01. PC indicates the expression of miR-221 and miR-222 in isolated mouse hepatocytes. #p<0.01 compared with stellate cells at day 7. (B) Expression of Col1A1 and α-smooth muscle actin (αSMA) mRNAs in mouse stellate cells during primary culture. Glyceraldehyde 3-phosphate dehydrogenase was used as an internal control. *p<0.05, **p<0.01. (C) Expression of miR-221 and miR-221 in HepG2, Huh7, NIH3T3 and LX-2. **p<0.01. (D and E) Regulation of miR-222 expression in mouse primary stellate cells. D: At 1 day after culture, the cells were treated with transforming growth factor α (TGFα; 1 or 10 ng/ml), tumour necrosis factor α (TNFα; 0.1 or 1 ng/ml), or 6-amino-4-(4-phenoxyphenylethylamono) quinazoline (QNZ; 10 or 100 nmol/l) for 24 h. Control indicates non-treated cells. **p<0.01 compared with control. E: At 1 day after culture, the cells were treated with TGFα (1 ng/ml), TNFα (0.1 ng/ml), QNZ (10 nmol/l), TGFα (1 ng/ml) plus QNZ (10 nmol/l), or TNFα (0.1 ng/ml) plus QNZ (10 nmol/l) for 72 h. Control indicates non-treated cells. *p<0.05, **p<0.01. (F) Morphology of mouse stellate cells observed under a microscope (×200) as in (E). (G) Expression of Col1A1 and αSMA mRNAs in mouse stellate cells treated with or without QNZ (10 nmol/l) during primary culture for 72 h.

programme in Japan has estimated that the annual incidence of HCC is 0.5–2.0% (mild liver fibrosis; F1/F2) and 5.3–7.9% (advanced liver fibrosis; (F3/F4) among patients with chronic hepatitis C.[39] miR-221 and miR-222, a pair of miRNAs encoded in a cluster on chromosome X, are overexpressed in a variety of human cancers, including HCC, in which they play oncogenic roles by downregulating p27, p57 and PTEN expression.[22 37 40] In particular, the pro-tumour activity of miR-221/222 is thought to be achieved by its regulation of CDKN1B (p27, Kip1).[41 42] In this study, we showed that miR-222 interacts with the *CDKN1B* 3′UTR and inhibits the expression of CDKN1B mRNA and protein in LX-2 cells, although it is unclear why increased miR-222 fails to affect the proliferation of stellate cells (figure 6). Type I interferon inhibits the proliferation of LX-2 cells by decreasing cyclin E and increasing p21 without affecting the expression of CDKN1B (p27).[31] In this regard, the proliferation of stellate cells may be strongly regulated by p21 rather than p27.

In general, miRNAs are transcribed by RNA polymerase II as part of capped and polyadenylated primary transcripts. The primary transcript is cleaved by the Drosha ribonuclease III to generate an approximately 70-nt stem-loop precursor miRNA, which is further cleaved by the cytoplasmic Dicer ribonuclease to generate the mature miRNA. In addition to this common pathway, recent investigations have shown that other factors are involved in the transcription of miRNAs by binding to their promoter regions. For instance, Galardi *et al* identified two separate regions upstream of the miR-221/222 promoter that are bound by the NF-κB subunit p65 and drive efficient transcription in luciferase reporter assays, indicating that the expression of miR-221/222 is induced by NF-κB activation in prostate carcinoma and glioblastoma cells.[33] Because NF-κB is involved in

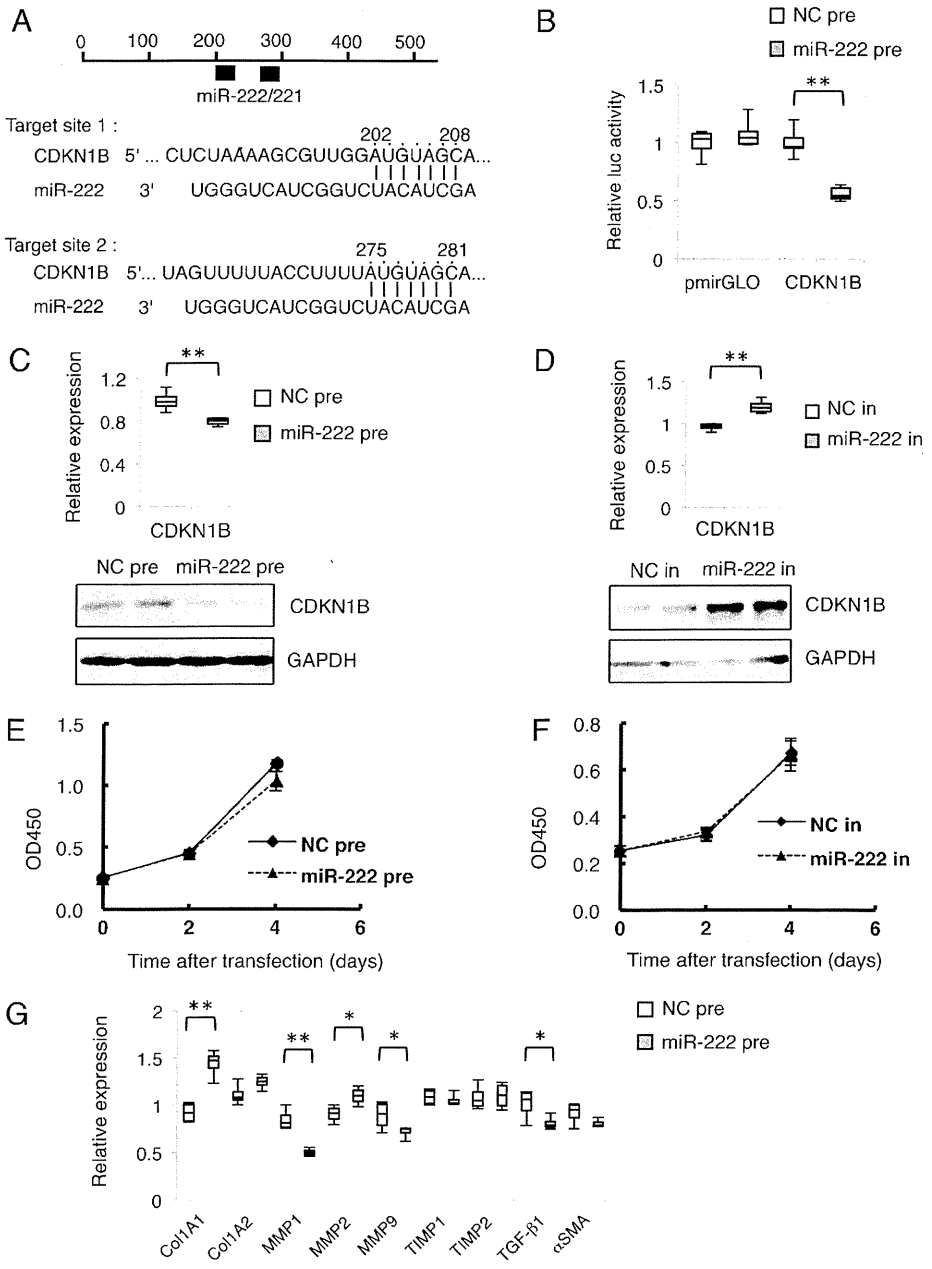

Figure 6 Interaction of miR-222 with the 3′UTR of CDKN1B mRNA. (A) Schematic indication of the miR-221/222 binding sites in the 3′UTR of CDKN1B mRNA based on TargetScan Human Release 5.1 (http://www.targetscan.org/). Black boxes indicate miR-221 or miR-222. Two predicted target sites of miR-221/222 are present in the 3′UTR of CDKN1B mRNA. (B) Reporter gene assay to test the interaction between the 3′UTR of CDKN1B mRNA and miR-222 in LX-2 cells. Relative luciferase activity derived from pCDKN1B—miR-222/mirGLO in the presence of miR-222 precursors. The pmirGLO vector was used as a negative control reporter vector. NC pre: co-transfection of reporter vectors together with a negative control miRNA precursor, which has a scrambled sequence. miR-222 pre: co-transfection of reporter vectors together with miR-222 precursors. The results are expressed relative to the activity in the presence of negative control precursors. **p<0.01. (C) Effect of miR-222 precursors on the expression of CDKN1B mRNA and protein in LX-2 cells. LX-2 cells were transfected with 50 nM miR-222 precursor (grey column) or a negative control (white column). At 24 h after transfection, CDKN1B mRNA (upper) and protein (lower) were measured. Glyceraldehyde 3-phosphate dehydrogenase (GAPDH) was used as an internal control. **p<0.01. (D) Effect of miR-222 inhibitors on the expression of CDKN1B mRNA and protein in LX-2 cells. LX-2 cells were transfected with 50 nM miR-222 inhibitor (grey column) or a negative control (white column). At 24 h after transfection, CDKN1B mRNA (upper) and protein (lower) were measured. GAPDH was used as an internal control. **p<0.01. (E, F) Effect of 50 nM miR-222 precursors (E) and inhibitors (F) on LX-2 cell growth, determined by WST-1 assay. (G) Effect of miR-222 precursors on the expression of fibrosis-related mRNAs in LX-2 cells. LX-2 cells were transfected with 50 nM miR-222 precursor (grey column) or a negative control (white column). At 24 h after transfection, the mRNAs were quantified. GAPDH was used as an internal control. *p<0.05, **p<0.01. ColA1, α1 (I) collagen; MMP, matrix metalloproteinase; αSMA, α-smooth muscle actin; TGFβ1, transforming growth factor β1; TIMP, tissue inhibitor of matrix metalloproteinase.

the process of stellate cell activation,[34–36] we speculated that the expression of miR-222 might be regulated through NF-κB activation in stellate cells. We found, however, that miR-222 expression was inhibited by QNZ, an NF-κB inhibitor, accompanied by the morphological maintenance of quiescence, and upregulated by the NF-κB activators TNFα and TGFα.

miRNA expression profiles can serve as useful tools for understanding and investigating the mechanism of the progression of liver fibrosis and can serve as new fibrosis biomarkers. miRNAs are packed into exosomes and circulate in blood.[43] However, this raises the question of whether circulating levels of miRNAs in blood correlate with the progression of liver fibrosis at the tissue level. Roderburg *et al* demonstrated that the expression levels of miR-29 family members in human liver fibrosis correlate with the downregulation of miR-29a in the serum.[38] Here, we observed that the expression of miR-222 in human livers with chronic trauma significantly correlated with the expression of Col1A1 mRNA, suggesting that miR-222 is a potential biomarker of liver fibrosis progression, although its utility as a serum biomarker needs further validation. Li *et al* recently reported that the miR-221 level in blood correlates with cirrhosis, tumour size and tumour stage and provides predictive value for prognosis in patients with HCC.[44]

This study has some limitations. The molecular mechanisms of liver fibrosis in viral hepatitis and in NASH may not exactly the same. In addition, fibrosis in human livers usually progresses

slowly, over the course of decades, so it is not practical to examine the expression of miRNAs at time points throughout progression. In contrast, liver fibrosis in experimental animals progresses quickly, so that within several weeks we could track the changes in miRNA expression at several time points. To establish the utility of miR-221/222 as biomarkers of liver fibrosis irrespective of aetiology, further studies are required to understand the exact mechanism by which the miRNAs participate in the progression of fibrosis.

In conclusion, we showed that miR-221 and miR-222 may be new markers for stellate cell activation and liver fibrosis progression in both humans and mice. These miRNAs could be used in the diagnosis of human liver fibrosis in clinical practice in the near future.

Acknowledgements We thank Drs Hiroyuki Motoyama, Le Thi Thanh Thuy, Masashi Iizuka and Tohru Komiya; Miss Shinobu Momen and Mrs Mami Mori for their valuable comments on this study.

Funding NK was supported by a grant-in-aid for scientific research from the Japan Society for the Promotion of Science (JSPS) (No 21390232; 2009—2011), a grant from the Ministry of Health, Labour and Welfare of Japan (2008—2010) and a Thrust Area Research Grant from Osaka City University (2008—2011). TO was supported by a grant-in-aid for scientific research from the JSPS (No 22790666; 2010—2011).

Competing interests None.

Ethics approval Ethics approval was provided by Osaka City University Medical School.

Contributors TO, EM, NK: conception, design, analysis and interpretation of data, drafting of the manuscript, critical revision of article, final approval given. HF, YS: analysis and interpretation of data, final approval given. KY, KI: conception, design, drafting of the manuscript, final approval given.

Provenance and peer review Not commissioned; externally peer reviewed.

REFERENCES

1. **Friedman SL.** Evolving challenges in hepatic fibrosis. *Nat Rev Gastroenterol Hepatol* 2010;**7**:425—36.
2. **Angulo P.** Nonalcoholic fatty liver disease. *N Engl J Med* 2002;**346**:1221—31.
3. **Matteoni CA,** Younossi ZM, Gramlich T, *et al.* Nonalcoholic fatty liver disease: a spectrum of clinical and pathological severity. *Gastroenterology* 1999;**116**:1413—19.
4. **Brunt EM,** Janney CG, Di Bisceglie AM, *et al.* Nonalcoholic steatohepatitis: a proposal for grading and staging the histological lesions. *Am J Gastroenterol* 1999;**94**:2467—74.
5. **Friedman SL.** Molecular regulation of hepatic fibrosis, an integrated cellular response to tissue injury. *J Biol Chem* 2000;**275**:2247—50.
6. **Kawada N.** Evolution of hepatic fibrosis research. *Hepatol Res* 2011;**41**:199—208.
7. **Wake K.** "Sternzellen" in the liver: perisinusoidal cells with special reference to storage of vitamin A. *Am J Anat* 1971;**132**:429—62.
8. **Filipowicz W,** Bhattacharyya SN, Sonenberg N. Mechanisms of post-transcriptional regulation by microRNAs: are the answers in sight? *Nat Rev Genet* 2008;**9**:102—14.
9. **Bartel DP.** MicroRNAs: genomics, biogenesis, mechanism and function. *Cell* 2004;**116**:281—97.
10. **Brennecke J,** Hipfner DR, Stark A, *et al.* bantam encodes a developmentally regulated microRNA that controls cell proliferation and regulates the proapoptotic gene hid in Drosophila. *Cell* 2003;**113**:25—36.
11. **Schratt GM,** Tuebing F, Nigh EA, *et al.* A brain-specific microRNA regulates dendritic spine development. *Nature* 2006;**439**:283—9.
12. **Chen CZ,** Li L, Lodish HF, *et al.* MicroRNAs modulate hematopoietic lineage differentiation. *Science* 2004;**303**:83—6.
13. **Kota J,** Chivukula RR, O'Donnell KA, *et al.* Therapeutic microRNA delivery suppresses tumorigenesis in a murine liver cancer model. *Cell* 2009;**137**:1005—17.
14. **Chen JF,** Murchison EP, Tang R, *et al.* Targeted deletion of Dicer in the heart leads to dilated cardiomyopathy and heart failure. *Proc Natl Acad Sci U S A* 2008;**105**:2111—16.
15. **Perkins DO,** Jeffries CD, Jarskog LF, *et al.* microRNA expression in the prefrontal cortex of individuals with schizophrenia and schizoaffective disorder. *Genome Biol* 2007;**8**:R27.
16. **Lewis AP,** Jopling CL. Regulation and biological function of the liver-specific miR-122. *Biochem Soc Trans* 2010;**38**:1553—7.
17. **Jopling CL,** Yi M, Lancaster AM, *et al.* Modulation of hepatitis C virus RNA abundance by a liver-specific MicroRNA. *Science* 2005;**309**:1577—81.
18. **Li YP,** Gottwein JM, Scheel TK, *et al.* MicroRNA-122 antagonism against hepatitis C virus genotypes 1-6 and reduced efficacy by host RNA insertion or mutations in the HCV 5' UTR. *Proc Natl Acad Sci U S A* 2011;**108**:4991—6.
19. **Lanford RE,** Hildebrandt-Eriksen ES, Petri A, *et al.* Therapeutic silencing of microRNA-122 in primates with chronic hepatitis C virus infection. *Science* 2010;**327**:198—201.
20. **Pedersen IM,** Cheng G, Wieland S, *et al.* Interferon modulation of cellular microRNAs as an antiviral mechanism. *Nature* 2007;**449**:919—22.
21. **Sarasin-Filipowicz M,** Krol J, Markiewicz I, *et al.* Decreased levels of microRNA miR-122 in individuals with hepatitis C responding poorly to interferon therapy. *Nat Med* 2009;**15**:31—3.
22. **Pineau P,** Volinia S, McJunkin K, *et al.* miR-221 overexpression contributes to liver tumorigenesis. *Proc Natl Acad Sci U S A* 2010;**107**:264—9.
23. **Marquez RT,** Bandyopadhyay S, Wendlandt EB, *et al.* Correlation between microRNA expression levels and clinical parameters associated with chronic hepatitis C viral infection in humans. *Lab Invest* 2010;**90**:1727—36.
24. **Bedossa P,** Poynard T. An algorithm for the grading of activity in chronic hepatitis C. The METAVIR Cooperative Study Group. *Hepatology* 1996;**24**:289—93.
25. **Sato F,** Tsuchiya S, Terasawa K, *et al.* Intra-platform repeatability and inter-platform comparability of microRNA microarray technology. *PLoS One* 2009;**4**:e5540.
26. **Ikejima K,** Honda H, Yoshikawa M, *et al.* Leptin augments inflammatory and profibrogenic responses in the murine liver induced by hepatotoxic chemicals. *Hepatology* 2001;**34**:288—97.
27. **Mu YP,** Ogawa T, Kawada N. Reversibility of fibrosis, inflammation and endoplasmic reticulum stress in the liver of rats fed a methionine-choline-deficient diet. *Lab Invest* 2010;**90**:245—56.
28. **Kristensen DB,** Kawada N, Imamura K, *et al.* Proteome analysis of rat hepatic stellate cells. *Hepatology* 2000;**32**:268—77.
29. **Xu L,** Hui AY, Albanis E, *et al.* Human hepatic stellate cell lines, LX-1 and LX-2: new tools for analysis of hepatic fibrosis. *Gut* 2005;**54**:142—51.
30. **Ogawa T,** Iizuka M, Sekiya Y, *et al.* Suppression of type I collagen production by microRNA-29b in cultured human stellate cells. *Biochem Biophys Res Commun* 2010;**391**:316—21.
31. **Sekiya Y,** Ogawa T, Iizuka M, *et al.* Down-regulation of cyclin E1 expression by microRNA-195 accounts for interferon-beta-induced inhibition of hepatic stellate cell proliferation. *J Cell Physiol* 2011;**226**:2535—42.
32. **Murakami Y,** Toyoda H, Tanaka M, *et al.* The progression of liver fibrosis is related with overexpression of the miR-199 and 200 families. *PLoS One* 2011;**6**:e16081.
33. **Galardi S,** Mercatelli N, Farace MG, *et al.* NF-kB and c-Jun induce the expression of the oncogenic miR-221 and miR-222 in prostate carcinoma and glioblastoma cells. *Nucleic Acids Res* 2011;**39**:3892—902.
34. **Lee KS,** Buck M, Houglum K, *et al.* Activation of hepatic stellate cells by TGF alpha and collagen type I is mediated by oxidative stress through c-myb expression. *J Clin Invest* 1995;**96**:2461—8.
35. **Rippe RA,** Schrum LW, Stefanovic B, *et al.* NF-kappaB inhibits expression of the alpha1(I) collagen gene. *DNA Cell Biol* 1999;**18**:751—61.
36. **Lang A,** Schoonhoven R, Tuvia S, *et al.* Nuclear factor kappaB in proliferation, activation and apoptosis in rat hepatic stellate cells. *J Hepatol* 2000;**33**:49—58.
37. **Fornari F,** Gramantieri L, Ferracin M, *et al.* MiR-221 controls CDKN1C/p57 and CDKN1B/p27 expression in human hepatocellular carcinoma. *Oncogene* 2008;**27**:5651—61.
38. **Roderburg C,** Urban GW, Bettermann K, *et al.* Micro-RNA profiling reveals a role for miR-29 in human and murine liver fibrosis. *Hepatology* 2011;**53**:209—18.
39. **Yoshida H,** Shiratori Y, Moriyama M, *et al.* Interferon therapy reduces the risk for hepatocellular carcinoma: national surveillance program of cirrhotic and noncirrhotic patients with chronic hepatitis C in Japan. IHIT Study Group. Inhibition of Hepatocarcinogenesis by Interferon Therapy. *Ann Intern Med* 1999;**131**:174—81.
40. **Garofalo M,** Di Leva G, Romano G, *et al.* miR-221&222 regulate TRAIL resistance and enhance tumorigenicity through PTEN and TIMP3 downregulation. *Cancer Cell* 2009;**16**:498—509.
41. **le Sage C,** Nagel R, Egan DA, *et al.* Regulation of the p27(Kip1) tumor suppressor by miR-221 and miR-222 promotes cancer cell proliferation. *Embo J* 2007;**26**:3699—708.
42. **Galardi S,** Mercatelli N, Giorda E, *et al.* miR-221 and miR-222 expression affects the proliferation potential of human prostate carcinoma cell lines by targeting p27Kip1. *J Biol Chem* 2007;**282**:23716—24.
43. **Kosaka N,** Iguchi H, Ochiya T. Circulating microRNA in body fluid: a new potential biomarker for cancer diagnosis and prognosis. *Cancer Sci* 2010;**101**:2087—92.
44. **Li J,** Wang Y, Yu W, *et al.* Expression of serum miR-221 in human hepatocellular carcinoma and its prognostic significance. *Biochem Biophys Res Commun* 2011;**406**:70—3.

Biochemical and Biophysical Research Communications 412 (2011) 74–79

Contents lists available at ScienceDirect

Biochemical and Biophysical Research Communications

journal homepage: www.elsevier.com/locate/ybbrc

Suppression of hepatic stellate cell activation by microRNA-29b

Yumiko Sekiya [a,b], Tomohiro Ogawa [a,b,1], Katsutoshi Yoshizato [a,b,c], Kazuo Ikeda [d], Norifumi Kawada [a,b,*]

[a] Department of Hepatology, Graduate School of Medicine, Osaka City University, Osaka, Japan
[b] Liver Research Center, Graduate School of Medicine, Osaka City University, Osaka, Japan
[c] PhoenixBio Co. Ltd., Hiroshima, Japan
[d] Department of Anatomy and Cell Biology, Graduate School of Medical Sciences, Nagoya City University, Aichi, Japan

ARTICLE INFO

Article history:
Received 6 July 2011
Available online 26 July 2011

Keywords:
α-Smooth muscle actin
c-fos
Focal adhesion kinase
Extracellular signal-regulated kinase
Akt
Liver fibrosis

ABSTRACT

MicroRNAs (miRNAs) participate in the regulation of cellular functions including proliferation, apoptosis, and migration. It has been previously shown that the miR-29 family is involved in regulating type I collagen expression by interacting with the 3′UTR of its mRNA. Here, we investigated the roles of miR-29b in the activation of mouse primary-cultured hepatic stellate cells (HSCs), a principal collagen-producing cell in the liver. Expression of miR-29b was found to be down-regulated during HSC activation in primary culture. Transfection of a miR-29b precursor markedly attenuated the expression of Col1a1 and Col1a2 mRNAs and additionally blunted the increased expression of α-SMA, DDR2, FN1, ITGB1, and PDGFR-β, which are key genes involved in the activation of HSCs. Further, overexpression of miR-29b led HSCs to remain in a quiescent state, as evidenced by their quiescent star-like cell morphology. Although phosphorylation of FAK, ERK, and Akt, and the mRNA expression of c-jun was unaffected, miR-29b overexpression suppressed the expression of c-fos mRNA. These results suggested that miR-29b is involved in the activation of HSCs and could be a candidate molecule for suppressing their activation and consequent liver fibrosis.

1. Introduction

Liver fibrosis is characterized by excessive accumulation of extracellular matrices (ECMs) and is a common feature of chronic liver injury. Hepatic stellate cells (HSCs) are considered to be the primary population that contributes to fibrogenic reactions by producing ECM in response to liver trauma. HSCs, which reside in the space of Disse outside the liver sinusoids, maintain a quiescent phenotype and store vitamin A under physiological conditions. When liver injury occurs, they become activated and trans-differentiate into myofibroblast-like cells, which are proliferative cells that lose their vitamin A droplets, express α-smooth muscle actin (α-SMA), and secrete profibrogenic mediators and ECM proteins [1,2]. Therefore, controlling the activation of the HSC population is considered a potential therapeutic target for liver fibrosis.

MicroRNAs (miRNAs) are endogenous, small, non-coding RNAs that work as post-transcriptional regulators of gene expression through their interaction with the 3′ untranslated region (3′UTR) of target mRNAs [3]. They participate in various biological phenomena, such as cell proliferation, development, differentiation, and metabolism [3]. Regarding HSCs, it was reported that miR-15b and miR-16 are down-regulated upon HSC activation and that their overexpression induces apoptosis and a delay in the cell cycle progression of HSCs [4,5]. Knockdown of miR-27a and miR-27b in activated HSCs reportedly allowed their reversion to a quiescent phenotype and decreased their rate of cell proliferation [6]. MiR-150 and miR-194 were reported to suppress proliferation, activation, and ECM production by HSCs [7]. We also reported the involvement of miR-195 in the proliferation of HSCs when treated with interferon [8].

Previously, we showed that miR-29b was induced by interferon treatment and that it suppressed type I collagen production in the human HSC line LX-2 [9]. Moreover, Roderburg et al. reported that miRNAs in the miR-29 family were significantly decreased in the

Abbreviations: BSA, bovine serum albumin; Col1a1, alpha 1 (I) collagen; Col1a2, alpha 2 (I) collagen; DDR, discoidin domain receptor; DAPI, 4′,6-diamidino-2-phenylindole; DMEM, Dulbecco's modified Eagle's medium; ECM, extracellular matrix; ERK, extracellular signal-regulated kinase; FAK, focal adhesion kinase; FBS, fetal bovine serum; FN, fibronectin; GAPDH, glyceraldehyde-3-phosphate dehydrogenase; HSC, hepatic stellate cell; ITGB1, integrin β1; miRNA, microRNA; PBS, phosphate buffered saline; PDGFR-β, platelet-derived growth factor receptor-β; PI3K, phosphatidylinositol-3 kinase; SDS, sodium dodecyl sulfate; α-SMA, α-smooth muscle actin; TGF-β, transforming growth factor-β; 3′UTR, 3′ untranslated region.

* Corresponding author. Address: Department of Hepatology, Graduate School of Medicine, Osaka City University, 1-4-3 Asahimachi, Abeno, Osaka 545-8585, Japan. Fax: +81 6 6646 6072.
E-mail address: kawadanori@med.osaka-cu.ac.jp (N. Kawada).
[1] Present address: Center for the Advancement of Higher Education, Faculty of Engineering, Kinki University, Hiroshima, Japan.

0006-291X/$ - see front matter © 2011 Elsevier Inc. All rights reserved.
doi:10.1016/j.bbrc.2011.07.041

fibrotic liver tissue of humans and mice [10]. Thus, it has been speculated that the change in the expression of miR-29 is closely related to the development of liver fibrosis. Although analyses of miR-29 functions were performed on ECM metabolism in these reports, the cells used in these experiments were immortalized cell lines that had already been activated and had become myofibroblastic, which does not always reflect miR-29 function in quiescent HSCs *in vivo*. Therefore, it is important to evaluate the effect of miR-29 on the activation of primary-cultured HSCs. These cells are known to undergo spontaneous activation and transdifferentiation into myofibroblastic cells in culture, similarly to those *in vivo*. Activated HSCs express α-SMA and produce fibrogenic mediators, such as type I collagen and transforming growth factor-β (TGF-β).

Here, we show the effects of miR-29b on the activation of HSCs using freshly isolated primary-cultured mouse HSCs. Overexpression of miR-29b suppressed cell viability and the expression of α-SMA. These effects seemed to be independent of the activation of focal adhesion kinase (FAK), extracellular signal-regulated kinase (ERK), and phosphatidylinositol-3 kinase (PI3K)–Akt, but were partially dependent on the reduction of c-fos mRNA.

2. Materials and methods

2.1. Cells

Primary HSCs were isolated from 12- to 16-week-old male C57BL/6N mice (Japan SLC Inc., Shizuoka, Japan) by pronase–collagenase digestion and subsequent purification by a single-step Nycodenz gradient, as previously described [11]. All animals received humane care, and the experimental protocol was approved by the Committee of Laboratory Animals according to institutional guidelines. Isolated HSCs were cultured on plastic dishes or glass chamber slides in Dulbecco's modified Eagle's medium (DMEM) (Sigma Chemical Co., St. Louis, MO, USA) supplemented with 10% fetal bovine serum (FBS) (Invitrogen, Carlsbad, CA, USA), 100 U/ml penicillin, and 100 μg/ml streptomycin. The purity of cultures was evaluated by observation of the characteristic stellate cell shape using phase-contrast microscopy.

The human HSC line LX-2 was donated by Dr. Scott L. Friedman (Mount Sinai School of Medicine, New York, NY, USA) [12]. LX-2 cells were maintained in DMEM as described above.

2.2. Transient transfection of a miR-29b precursor

The miR-29b precursor (Ambion, Austin, TX, USA), which was a double-strand RNA mimicking the endogenous miR-29b precursor, and a negative control (Ambion) were transfected into mouse HSCs and LX-2 cells using Lipofectamine RNAiMAX (Invitrogen) at a final concentration of 10 nM in accordance with the manufacturer's instructions. Briefly, the miRNA precursor and Lipofectamine RNAiMAX were mixed at a ratio of 5 (pmol):1 (μl) in Opti-MEM I Reduced Medium (Invitrogen), incubated for 20 min at room temperature, and then added to the cultures.

2.3. Quantitative real-time PCR

Total RNA was extracted from cells using the miRNeasy Mini Kit (Qiagen, Valencia, CA, USA). Fifty nanograms of total RNA was reverse-transcribed to cDNA using the ReverTra Ace qPCR RT Kit (Toyobo, Osaka, Japan) in accordance with the manufacturer's instructions. Gene expression was measured by real-time PCR using cDNA, SYBR Green real-time PCR Master Mix (Toyobo), and a set of gene-specific oligonucleotide primers [alpha 1 (I) collagen (Col1a1): forward 5′-CCTGGCAAAGACGGACTCAAC-3′, reverse 5′-GCTGAAGT CATAACCGCCACTG-3′; alpha 2 (I) collagen (Col1a2): forward 5′-AA GGGTCCCTCTGGAGAACC-3′, reverse 5′-TCTAGAGCCAGGGAG AC-CCA-3′; α-SMA: forward 5′-TCCCTGGAGAAGAGCTACGAACT-3′, reverse 5′-AAGCGTTCGTTTCCAATGGT-3′; discoidin domain receptor (DDR) 2: forward 5′-CGAAAGCTTCCAGAGTTTGC-3′, reverse 5′-GCT TCACAACACCACTGCAC-3′; fibronectin (FN) 1: forward 5′-GATGCC GATCAGAAGTTTGG-3′, reverse 5′-GGTTGTGCAGATCTCCTCGT-3′; β1 integrin (ITGB1): forward 5′-CAACCACAACAGCTGCTTCTAA-3′, reverse 5′-TCAGCCCTCTTGAATTTTAATGT-3′; platelet-derived growth factor receptor-β (PDGFR-β): forward 5′-GCGTATCTATATCT TTGTGCCAGA-3′, reverse 5′-ACAGGTCCTCGGAG TCCAT-3′; c-fos: forward 5′-AGAAGGGGCAAAGTAGAGCA-3′, reverse 5′-CAGCTCC CTCCTCCGATT-3′; c-jun: forward 5′-CCAGAAGATGGTGTGGTGTTT-3′, reverse 5′-CTGACCCTCTCCCCTTGC-3′; glyceraldehyde-3-phosphate dehydrogenase (GAPDH): forward 5′-TGCACCACCAACTGCT-TAG-3′, reverse 5′-GGATGCAGGGATGATGTTC-3′] using an Applied Biosystems Prism 7500 (Applied Biosystems, Foster City, CA, USA). To detect miR-29b expression, the reverse transcription reaction was performed using a TaqMan microRNA Assay (Applied Biosystems) in accordance with the manufacturer's instructions. The expression level of GAPDH was used to normalize the relative abundance of mRNAs and miR-29b.

2.4. Immunoblots

Cells were lysed in RIPA buffer [50 mM Tris/HCl, pH7.5, 150 mM NaCl, 1% NP-40, 0.5% sodium deoxycholate, 0.1% sodium dodecyl sulfate (SDS)] containing Protease Inhibitor Cocktail, Phosphatase Inhibitor Cocktail 1, and Phosphatase Inhibitor Cocktail 2 (Sigma). Proteins (2.5–10 μg) were electrophoresed in a 5–20% gradient SDS–polyacrylamide gel (ATTO Co., Tokyo, Japan) and were then transferred onto Immobilon P membranes (Millipore, Bedford, MA, USA). After blocking, the membranes were incubated with primary antibodies [mouse monoclonal antibody against α-SMA (Dako, Ely, UK); rabbit polyclonal antibody against type I collagen (Rockland Immunochemicals, Inc., Gilbertsville, PA, USA); rabbit polyclonal antibodies against PDGFR-β and GAPDH (Santa Cruz Biotechnology Inc., Santa Cruz, CA, USA); rabbit polyclonal antibodies against FAK and phospho-FAK (Y397) (Cell Signaling Technology Inc., Beverly, MA, USA); and mouse monoclonal antibodies against ERK, phospho-ERK (T202/Y204), Akt, and phospho-Akt (S473) (Cell Signaling Technology Inc.)] followed by peroxidase-conjugated secondary antibodies (Dako). Immunoreactive bands were visualized by the enhanced chemiluminescence system (Amersham, Roosdaal, Netherlands) using a Fujifilm Image Reader LAS-3000 (Fuji Medical Systems, Stamford, CT, USA).

2.5. F-actin staining

HSCs on glass chamber slides were fixed in 4% paraformaldehyde in phosphate buffered saline (PBS) for 30 min and were permeabilized with 0.1% Triton X-100 in PBS for 5 min at room temperature. The nonspecific background signal was blocked with 1% bovine serum albumin (BSA) in PBS for 20 min. F-actin was stained with MFP488-phalloidin (Mobitec, Goettingen, Germany) in PBS with 1% BSA for 20 min. 4′,6-diamidino-2-phenylindole (DAPI) (Dojindo Laboratories, Kumamoto, Japan) was used for counterstaining.

2.6. Cell viability assay

The cell viability was evaluated by the WST-1 assay based changes in absorbance at 450 nm. Freshly isolated mouse HSCs or LX-2 cells were plated in 96-well plates at a density of 1.5×10^4 or 3×10^3 cells/well, respectively. The following day, cells were transfected with the miR-29b precursor or a negative

control as described above and were incubated for an additional 3 or 5 days before the assessment of cell viability. In another experiment, mouse HSCs that were transfected with the miR-29b precursor the day before were serum-starved overnight and then stimulated with PDGF-BB (10 ng/ml) (R&D Systems, Minneapolis, MO, USA). After incubation for 3 days, cell viability was assessed by the WST-1 assay.

2.7. Statistical analysis

Data presented as bar graphs are the means ± SD of at least three independent experiments. Statistical analysis was performed using the Student's *t*-test, and $P < 0.05$ was considered to be statistically significant.

3. Results and discussion

3.1. Expression of miR-29b in mouse HSCs during spontaneous activation

At 1 day of culture after isolation, mouse HSCs adhered to plastic plates and exhibited round cell bodies with numerous lipid droplets similar to those observed in lipocytes (Fig. 1A). Cell bodies then began to gradually spread and flatten, increasing in size, and losing lipid droplets, resulting in the activated myofibroblastic phenotype (Fig. 1A). In addition to the changes in cell appearance, mRNA expression levels of α-SMA, Col1a1, Col1a2, FN1, DDR2, ITGB1, and PDGFR-β significantly increased at Days 4 and 7 of culture as compared to Day 1 (Fig. 1B). Immunoblot analyses confirmed the increases of type I collagen, α-SMA, and PDGFR-β protein levels at Days 4 and 7 (Fig. 1C). These molecules have already been reported to be up-regulated in activated HSCs and involved in fibrosis [2]. Thus, the primary mouse HSCs used in this study were in an activated state. Although TGF-β1 is known as a key regulator of collagen production and fibrosis [13], its mRNA expression level in mouse HSCs remained unchanged due to an unknown reason in this study (Fig. 1B). In contrast, miR-29b expression in mouse HSCs was significantly decreased to 28% and 32% at Days 4 and 7, respectively, as compared to Day 1 (Fig. 1D). These findings raised the possibility that a reduction in miR-29b contributed to the up-regulation of the fibrosis-related genes listed above.

3.2. Effects of miR-29b overexpression on the activation of HSCs

To investigate this possibility, we next examined the effects of miR-29b overexpression on the activation of HSCs. Overexpression of miR-29b was achieved by the transient transfection of a synthesized miR-29b precursor, which was a double-strand RNA mimicking the endogenous miR-29b precursor. As shown in Fig. 2A, transfection of the miR-29b precursor markedly suppressed mRNA expression of Col1a1 and Col1a2 to 8% and 18%, respectively. Transfection significantly reduced mRNA expression of FN1 to 61% and also affected the expression of HSC activation-related molecules, such as α-SMA, DDR2, ITGB1, and PDGFR-β to 57%, 62%, 73%, and

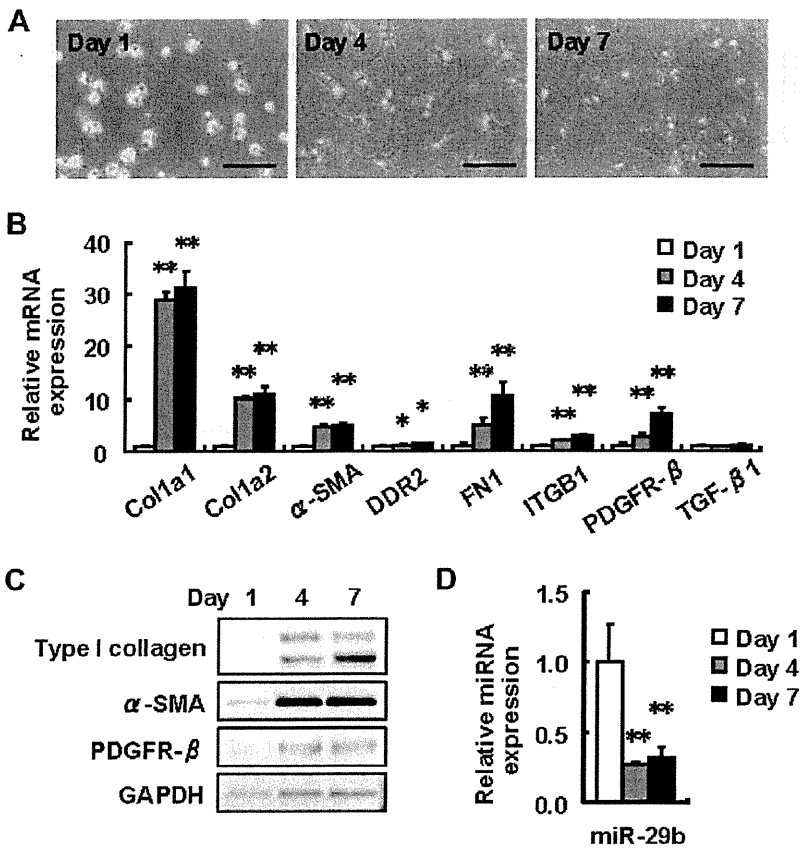

Fig. 1. Expression of miR-29b in mouse primary HSCs during culture. HSCs were isolated from mouse liver (Day 0) and cultured for the indicated periods. (A) Phase-contrast microscopy. Scale bar, 200 μm. (B) mRNA expression levels of Col1a1, Col1a2, α-SMA, DDR2, FN1, ITGB1, PDGFR-β and TGF-β1 were analyzed by real-time PCR. Results are expressed as relative expression against the expression on Day 1 of corresponding genes. $^{*}P < 0.05$, $^{**}P < 0.01$ compared with Day 1. (C) Protein expression levels of type I collagen, α-SMA and PDGFR-β were analyzed by Western blot. GAPDH served as an internal control. (D) miR-29b expression level was analyzed by real-time PCR. $^{*}P < 0.05$, $^{**}P < 0.01$ compared with Day 1.

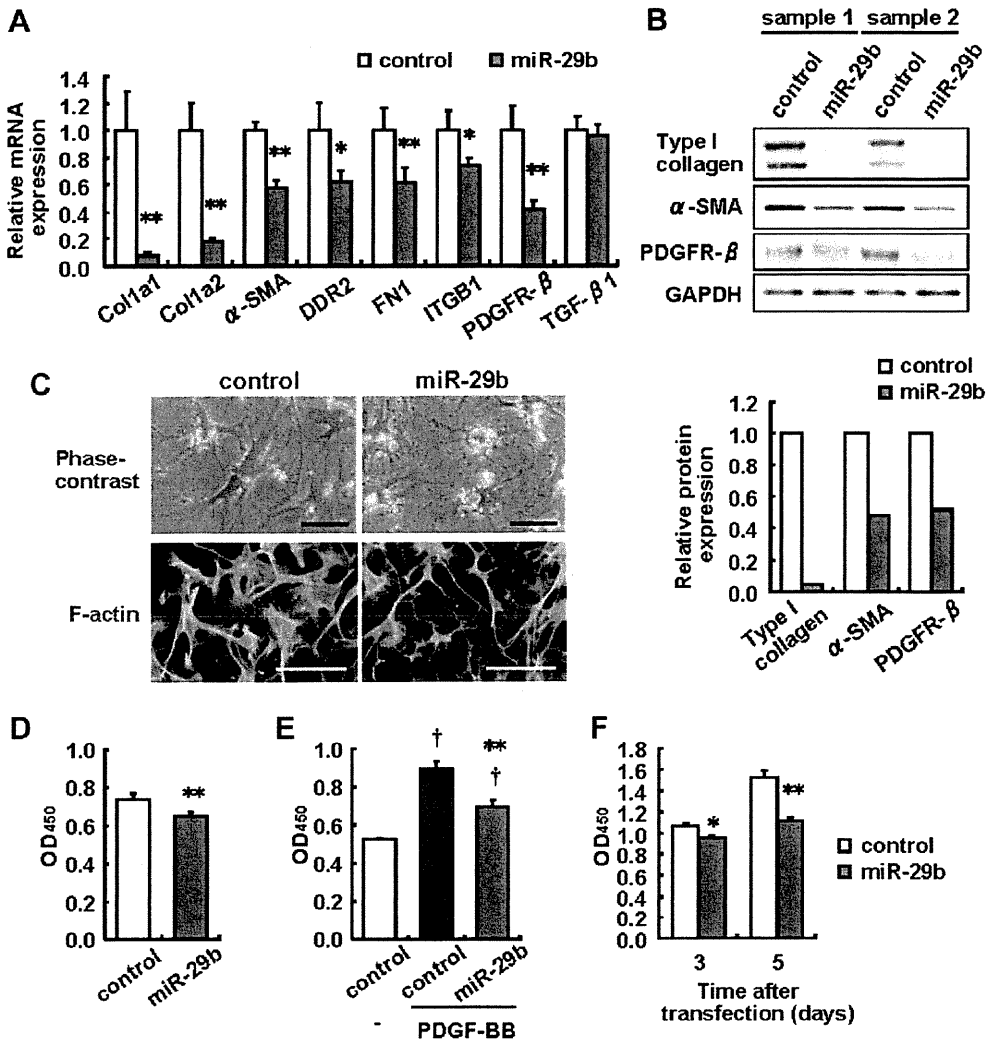

Fig. 2. Effects of miR-29b overexpression on the activation of HSCs. (A–D) Mouse HSCs were transfected with 10 nM miR-29b precursor or a negative control (control) on Day 1 and incubated for 3 days. (A) mRNA expression levels of Col1a1, Col1a2, α-SMA, DDR2, FN1, ITGB1, PDGFR-β and TGF-β1 were analyzed by real-time PCR. The results are expressed as relative expression against the expression of untreated control. $^{*}P < 0.05$, $^{**}P < 0.01$ compared with control. (B) Protein expression levels of type I collagen, α-SMA and PDGFR-β were analyzed by Western blot. GAPDH served as an internal control. The lower graph indicates the densitometric results of $n = 2$. (C) Phase-contrast microscopy (upper) and MFP488-phalloidin staining for F-actin (lower). Scale bar, 100 μm. (D) Cell viability was evaluated by WST-1 assay. $^{**}P < 0.01$ compared with control. (E) Mouse HSCs were transfected with miR-29b precursor or a negative control (control) on Day 1. Twenty-four hours later, cells were serum-starved overnight, stimulated with or without PDGF-BB (10 ng/ml) and incubated for an additional 3 days. In Day 6, cell viability was evaluated by WST-1 assay. $^{**}P < 0.01$ compared with control plus PDGF-BB. $^{\dagger}P < 0.05$ compared with control plus non-treat. (F) LX-2 cells were transfected with miR-29b precursor or a negative control (control) and incubated for the indicated periods. Cell viability was evaluated by WST-1 assay. $^{*}P < 0.05$, $^{**}P < 0.01$ compared with the control.

42%, respectively. The TGF-β1 mRNA level was unaffected. At the protein level, expression of type I collagen, α-SMA, and PDGFR-β was suppressed by the overexpression of the miR-29b precursor (Fig. 2B). Col1a1, Col1a2, ITGB1, and PDGFR-β are predicted targets of miR-29b according to the miRNA target prediction databases TargetScan (http://www.targetscan.org/), miRBase (http://www.mirbase.org/), and mircrorna.org (http://www.microrna.org). Therefore, the suppression of these proteins might be due to the direct interaction of miR-29b with the 3′UTR of their corresponding mRNAs. Although α-SMA, DDR2, and FN1 are not predicted targets of miR-29b, their mRNA levels were suppressed. Thus, this effect was thought to be a secondary action of miR-29b over-expression. That is, it is suggested that miR-29b can not only target Col1a1, Col1a2, ITGB1, and PDGFR-β, but can also suppress the activation of HSCs by regulating other unidentified mechanisms, resulting in the suppression of α-SMA, DDR2, and FN1. In support of these results, morphological transformation from the quiescent to the myofibroblastic cell shape, as shown in Fig. 1A, was impeded in miR-29b precursor-transfected cells (Fig. 2C); miR-29b precursor-transfected cells exhibited star-like morphology with small cell bodies and slender dendritic processes as compared to negative control-transfected cells at Day 4. Staining with MFP-phalloidin, which labels F-actin, also confirmed cytoskeletal changes in miR-29b precursor-transfected HSCs. Taken together; these results suggest that miR-29b is able to suppress HSC activation as well as ECM expression.

3.3. Effect of miR-29b overexpression on number of HSCs

Activated HSCs are known to acquire proliferation abilities [1,2]. We considered the possibility that miR-29b was able to regulate the number of HSCs. As shown by the WST-1 assay, when the miR-29b precursor was transfected into HSCs at Day 1, the cell number observed at Day 4 was significantly reduced to 88% of the negative control-transfected cells (Fig. 2D). Treatment of HSCs with 10 ng/mL PDGF-BB, a key mitogen for HSCs [14], significantly

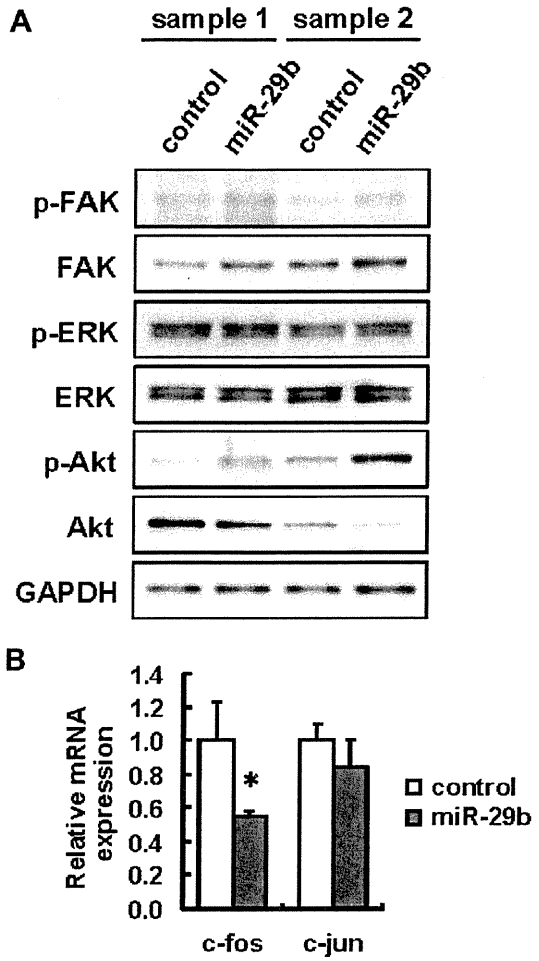

Fig. 3. Effects of miR-29b overexpression on the ECM- and growth factor-related signaling in mouse primary HSCs. Mouse HSCs were transfected with 10 nM miR-29b precursor or a negative control (control) on Day 1 and were incubated for 3 days. (A) Phosphorylation of FAK (Y397), ERK (T202/Y204) and Akt (S473) was analyzed by Western blot. (B) mRNA expression levels of c-fos and c-jun were analyzed by real-time PCR. The results are expressed as relative expression against the expression of control. $^*P < 0.05$ compared with control.

increased the cell number up to 1.7 times that of the non-treated cells (Fig. 2E), whereas overexpression of miR-29b inhibited this increase. Furthermore, in LX-2 cells, transfection of the miR-29b precursor decreased cell viability to 89% and 81% at 3 and 5 days following transfection, respectively (Fig. 2F). These results suggested that miR-29b is able to suppress the proliferation of HSCs and that down-regulation of miR-29b during HSC activation may contribute to their active proliferation.

3.4. Effects of miR-29b overexpression on the ECM- and growth factor-related signaling in primary mouse HSCs

The question of how miR-29b functions in blocking HSC activation was also examined. We showed that overexpression of miR-29b suppressed Col1a1, Col1a2, FN1, DDR2, ITGB1, and PDGFR-β expression (Fig. 2A and B). DDR2 is a receptor tyrosine kinase that is activated by the binding of collagen and was reported to be involved in the proliferation of HSCs and in the expression of matrix metalloproteinase-2 [15,16]. ITGB1 is a member of the integrin family and works as a FN or collagen receptor by forming a heterodimer with the integrin α subunit. ITGB1 is reported to be involved in the production of type I collagen and monocyte chemotactic protein-1 in HSCs [17,18]. PDGFR-β is a receptor of PDGF and is involved in the proliferation of activated HSCs [19,20]. Because it is known that intracellular signaling molecules such as FAK, ERK, and PI3K/Akt are key mediators for DDR2, ITGB1, and PDGFR-β [14,21–24], their down-regulation by miR-29b may affect downstream signaling, resulting in the inhibition of both activation and proliferation of HSCs. To verify this hypothesis, we investigated the effect of miR-29b overexpression on the activation of FAK, Akt, and ERK. Activation of these kinases was evaluated by immunoblot analyses to detect the phosphorylation of each protein. Unexpectedly, phosphorylation of FAK, ERK, and Akt was unaffected by miR-29b overexpression (Fig. 3A). Next, we also examined the mRNA expression of c-fos and c-jun, which form the transcription factor AP-1 complex and are located downstream of these signal kinases. Although transfection of the miR-29b precursor failed to alter c-jun expression, it significantly reduced c-fos mRNA expression to 55% (Fig. 3B). Because AP-1 is known to be one of the key transcription factors for the initiation of HSC activation [25,26], this fact indicates that effects of miR-29b may be partially mediated by c-fos down-regulation.

4. Conclusion

We confirmed that miR-29b expression decreased during HSC activation and found that overexpression of miR-29b is able to attenuate the activation and trans-differentiation of HSCs, although the precise molecular mechanism for this effect remains unknown. Changes in miR-29b expression seem to profoundly affect the activation of HSCs.

Conflict of interest

The authors have no conflict of interest to declare.

Acknowledgment

This work was supported by a grant from the Ministry of Health, Labor and Welfare of Japan to N. Kawada (2008–2010).

References

[1] R. Bataller, D.A. Brenner, Hepatic stellate cells as a target for the treatment of liver fibrosis, Semin. Liver Dis. 21 (2001) 437–451.
[2] S.L. Friedman, Molecular regulation of hepatic fibrosis an integrated cellular response to tissue injury, J. Biol. Chem. 275 (2000) 2247–2250.
[3] D.P. Bartel, MicroRNAs: genomics, biogenesis, mechanism, and function, Cell 116 (2004) 281–297.
[4] C.J. Guo, Q. Pan, B. Jiang, G.Y. Chen, D.G. Li, Effects of upregulated expression of microRNA-16 on biological properties of culture-activated hepatic stellate cells, Apoptosis 14 (2009) 1331–1340.
[5] C.J. Guo, Q. Pan, D.G. Li, H. Sun, B.W. Liu, miR-15b and miR-16 are implicated in activation of the rat hepatic stellate cell: an essential role for apoptosis, J. Hepatol. 50 (2009) 766–778.
[6] J.L. Ji, J.S. Zhang, G.C. Huang, J. Qian, X.Q. Wang, S. Mei, Over-expressed microRNA-27a and 27b influence fat accumulation and cell proliferation during rat hepatic stellate cell activation, FEBS Lett. 583 (2009) 759–766.
[7] S.K. Venugopal, J. Jiang, T.H. Kim, Y. Li, S.S. Wang, N.J. Torok, J. Wu, M.A. Zern, Liver fibrosis causes downregulation of miRNA-150 and miRNA-194 in hepatic stellate cells, and their overexpression causes decreased stellate cell activation, Am. J. Physiol. Gastrointest. Liver Physiol. 298 (2010) G101–G106.
[8] Y. Sekiya, T. Ogawa, M. Iizuka, K. Yoshizato, K. Ikeda, N. Kawada, Down-regulation of cyclin E1 expression by microRNA-195 accounts for interferon-β-induced inhibition of hepatic stellate cell proliferation, J. Cell. Physiol. 2010, doi:10.1002/jcp22598.
[9] T. Ogawa, M. Iizuka, Y. Sekiya, K. Yoshizato, K. Ikeda, N. Kawada, Suppression of type I collagen production by microRNA-29b in cultured human stellate cells, Biochem. Biophys. Res. Commun. 391 (2010) 316–321.
[10] C. Roderburg, G.W. Urban, K. Bettermann, M. Vucur, H. Zimmermann, S. Schmidt, J. Janssen, C. Koppe, P. Knolle, M. Castoldi, F. Tacke, C. Trautwein, T. Luedde, Micro-RNA profiling reveals a role for miR-29 in human and murine liver fibrosis, Hepatology 53 (2011) 209–218.

[11] N. Uyama, L. Zhao, E. Van Rossen, Y. Hirako, H. Reynaert, D.H. Adams, Z. Xue, Z. Li, R. Robson, M. Pekny, A. Geerts, Hepatic stellate cells express synemin, a protein bridging intermediate filaments to focal adhesions, Gut 55 (2006) 1276–1289.

[12] L. Xu, A.Y. Hui, E. Albanis, M.J. Arthur, S.M. O'Byrne, W.S. Blaner, P. Mukherjee, S.L. Friedman, F.J. Eng, Human hepatic stellate cell lines, LX-1 and LX-2: new tools for analysis of hepatic fibrosis, Gut 54 (2005) 142–151.

[13] D.M. Bissell, D. Roulot, J. George, Transforming growth factor beta and the liver, Hepatology 34 (2001) 859–867.

[14] F. Marra, M. Pinzani, R. Defranco, G. Laffi, P. Gentilini, Involvement of phosphatidylinositol 3-kinase in the activation of extracellular signal-regulated kinase by PDGF in hepatic stellate cells, FEBS Lett. 376 (1995) 141–145.

[15] E. Olaso, K. Ikeda, F.J. Eng, L.M. Xu, L.H. Wang, H.C. Lin, S.L. Friedman, DDR2 receptor promotes MMP-2-mediated proliferation and invasion by hepatic stellate cells, J. Clin. Invest. 108 (2001) 1369–1378.

[16] E. Olaso, J.P. Labrador, L.H. Wang, K. Ikeda, F.J. Eng, R. Klein, D.H. Lovett, H.C. Lin, S.L. Friedman, Discoidin domain receptor 2 regulates fibroblast proliferation and migration through the extracellular matrix in association with transcriptional activation of matrix metalloproteinase-2, J. Biol. Chem. 277 (2002) 3606–3613.

[17] F. Marra, S. Pastacaldi, R.G. Romanelli, M. Pinzani, P. Ticali, V. Carloni, G. Laffi, P. Gentilini, Integrin-mediated stimulation of monocyte chemotactic protein-1 expression, FEBS Lett. 414 (1997) 221–225.

[18] D.R. Wang, M. Sato, L.N. Li, M. Miura, N. Kojima, H. Senoo, Stimulation of pro-MMP-2 production and activation by native form of extracellular type I collagen in cultured hepatic stellate cells, Cell Struct. Funct. 28 (2003) 505–513.

[19] E. Borkham-Kamphorst, J. Herrmann, D. Stoll, J. Treptau, A.M. Gressner, R. Weiskirchen, Dominant-negative soluble PDGF-beta receptor inhibits hepatic stellate cell activation and attenuates liver fibrosis, Lab. Invest. 84 (2004) 766–777.

[20] C.G. Lechuga, Z.H. Hernandez-Nazara, E. Hernandez, M. Bustamante, G. Desierto, A. Cotty, N. Dharker, M. Choe, M. Rojkind, PI3K is involved in PDGF-beta receptor upregulation post-PDGF-BB treatment in mouse HSC, Am, J. Physiol. Gastrointest. Liver Physiol. 291 (2006) G1051–G1061.

[21] V. Carloni, R.G. Romanelli, M. Pinzani, G. Laffi, P. Gentilini, Focal adhesion kinase and phospholipase C gamma involvement in adhesion and migration of human hepatic stellate cells, Gastroenterology 112 (1997) 522–531.

[22] C. Rodriguez-Juan, P. de la Torre, I. Garcia-Ruiz, T. Diaz-Sanjuan, T. Munoz-Yague, E. Gomez-Izquierdo, P. Solis-Munoz, J.A. Solis-Herruzo, Fibronectin increases survival of rat hepatic stellate cells – a novel profibrogenic mechanism of fibronectin, Cell. Physiol. Biochem. 24 (2009) 271–282.

[23] H.J. Wu, Z.Q. Zhang, B. Yu, S. Liu, K.R. Qin, L.A. Zhu, Pressure activates Src-dependent FAK–Akt and ERK1/2 signaling pathways in rat hepatic stellate cells, Cell. Physiol. Biochem. 26 (2010) 273–280.

[24] K. Ikeda, L.H. Wang, R. Torres, H. Zhao, E. Olaso, F.J. Eng, P. Labrador, R. Klein, D. Lovett, G.D. Yancopoulos, S.L. Friedman, H.C. Lin, Discoidin domain receptor 2 interacts with Src and Shc following its activation by type I collagen, J. Biol. Chem. 277 (2002) 19206–19212.

[25] R. Gao, D.K. Ball, B. Perbal, D.R. Brigstock, Connective tissue growth factor induces c-fos gene activation and cell proliferation through p44/42 MAP kinase in primary rat hepatic stellate cells, J. Hepatol. 40 (2004) 431–438.

[26] J.E. Poulos, J.D. Weber, J.M. Bellezzo, A.M.D. Bisceglie, R.S. Britton, B.R. Bacon, J.J. Baldassare, Fibronectin and cytokines increase JNK, ERK, AP-1 activity, and transin gene expression in rat hepatic stellate cells, Am. J. Physiol. 273 (1997) G804–G811.

Journal of Cellular Physiology

Down-Regulation of Cyclin E1 Expression by MicroRNA-195 Accounts for Interferon-β-Induced Inhibition of Hepatic Stellate Cell Proliferation

YUMIKO SEKIYA,[1,2] TOMOHIRO OGAWA,[1,2] MASASHI IIZUKA,[1,2] KATSUTOSHI YOSHIZATO,[1,2,3] KAZUO IKEDA,[4] AND NORIFUMI KAWADA[1,2]*

[1]*Department of Hepatology, Graduate School of Medicine, Osaka City University, Osaka, Japan*

[2]*Liver Research Center, Graduate School of Medicine, Osaka City University, Osaka, Japan*

[3]*PhoenixBio Co. Ltd., Hiroshima, Japan*

[4]*Department of Anatomy and Cell Biology, Graduate School of Medical Sciences, Nagoya City University, Aichi, Japan*

Recent studies have suggested that interferons (IFNs) have an antifibrotic effect in the liver independent of their antiviral effect although its detailed mechanism remains largely unknown. Some microRNAs have been reported to regulate pathophysiological activities of hepatic stellate cells (HSCs). We performed analyses of the antiproliferative effects of IFNs in HSCs with special regard to microRNA-195 (miR-195). We found that miR-195 was prominently down-regulated in the proliferative phase of primary-cultured mouse HSCs. Supporting this fact, IFN-β induced miR-195 expression and inhibited the cell proliferation by delaying their G1 to S phase cell cycle progression in human HSC line LX-2. IFN-β down-regulated cyclin E1 and up-regulated p21 mRNA levels in LX-2 cells. Luciferase reporter assay revealed the direct interaction of miR-195 with the cyclin E1 3′UTR. Overexpression of miR-195 lowered cyclin E1 mRNA and protein expression levels, increased p21 mRNA and protein expression levels, and inhibited cell proliferation in LX-2 cells. Moreover miR-195 inhibition restored cyclin E1 levels that were down-regulated by IFN-β. In conclusion, IFN-β inhibited the proliferation of LX-2 cells by delaying cell cycle progression in G1 to S phase, partially through the down-regulation of cyclin E1 and up-regulation of p21. IFN-induced miR-195 was involved in these processes. These observations reveal a new mechanistic aspect of the antifibrotic effect of IFNs in the liver.

J. Cell. Physiol. 226: 2535–2542, 2011.

Hepatic fibrosis is characterized by excessive accumulation of extracellular matrices (ECM) and is a common feature of chronic liver diseases. Hepatic stellate cells (HSCs) are considered to play multiple roles in the fibrotic process. HSCs maintain a quiescent phenotype and store vitamin A under physiological conditions. When liver injury occurs, they become activated and trans-differentiate into myofibroblastic cells, whose characteristics include the proliferation, loss of vitamin A droplets, expression of α-smooth muscle actin (α-SMA), secretion of profibrogenic mediators and ECM (Friedman, 2000; Bataller and Brenner, 2001). Therefore, controlling the population and activation of HSCs should be a potential therapeutic target against liver fibrosis.

Interferons (IFNs) are cytokines with antiviral, immunomodulatory, and cell growth inhibitory effects. IFN-α and -β are classified as type I IFNs (Pestka et al., 1987; Uze et al., 2007), which are generally applied for the therapy of eradication of hepatitis B and C viruses. Studies using rodent models and cultured HSCs have also suggested that IFNs have a direct antifibrotic potential independently of their antivirus activity (Mallat et al., 1995; Fort et al., 1998; Shen et al., 2002; Inagaki et al., 2003; Chang et al., 2005; Tanabe et al., 2007; Ogawa et al., 2009), although the detailed molecular mechanisms of these effects of IFNs remain to be clarified.

Recently, microRNAs (miRNAs), which are endogenous small non-coding RNA, have become a focus of interest as post-transcriptional regulators of gene expression through interaction with the 3′ untranslated region (3′UTR) of target mRNAs (Bartel, 2004). miRNAs are known to participate in cell proliferation, development, differentiation, and metabolism (Bartel, 2004). Moreover, it has been reported that expression of miRNAs could alter hepatic pathophysiology; microRNA-122 (miR-122) is involved in the IFN-β-related defense system against viral hepatitis C (Pedersen et al., 2007), and miR-26 is associated with survival and response to adjuvant IFN-α therapy in patients with hepatocellular carcinoma (HCC) (Ji et al., 2009a). Regarding HSCs, miR-15b and miR-16 are down-regulated upon HSC's activation, and their overexpression induces apoptosis and a delay in the cell cycle (Guo et al., 2009a,b). Knockdown of miR-27a and miR-27b in activated HSCs allowed a switch to a more quiescent phenotype and decreased cell proliferation (Ji et al., 2009b). miR-150 and miR-194 suppress proliferation, activation, and ECM production of HSCs (Venugopal et al., 2010). Recently, we showed that miR-29b was induced by IFN and suppressed type I collagen production in LX-2 cells (Ogawa et al., 2010).

In the present study, we measured the levels of miR-195 in primary-cultured mouse HSCs and found that its expression was markedly reduced in their activation phase, suggesting the regulatory role of miR-195 in the activation/deactivation process of

Contract grant sponsor: The Ministry of Health, Labour and Welfare of Japan;
Contract grant number: 2008-KAKEN-IPPAN-003.

*Correspondence to: Norifumi Kawada, Department of Hepatology, Graduate School of Medicine, Osaka City University, 1-4-3, Asahimachi, Abeno, Osaka 545-8585, Japan.
E-mail: kawadanori@med.osaka-cu.ac.jp

Received 6 September 2010; Accepted 3 December 2010

Published online in Wiley Online Library (wileyonlinelibrary.com), 29 December 2010.
DOI: 10.1002/jcp.22598

TABLE 1. Sequences of primers used in real-time PCR analyses and 3'UTR cloning for luciferase reporter assay

Gene	Accession no.	Sequence
Real-time PCR		
CDK2	NM_001798	Forward: 5'-CTCCACCGAGACCTTAAACCTCAG-3' Reverse: 5'-TCGGTACCACAGGGTCACCA-3'
CDK4	NM_000075	Forward: 5'-GATAGATGCTGACCCATACCTCAAG-3' Reverse: 5'-ATGCTGTGGTGCTTTGAGGTAG-3
CDK6	NM_001259	Forward: 5'-ATATCTGCCTACAGTGCCCTGTCTC-3' Reverse: 5'-GTGGGAATCCAGGTTTTCTTTGCAC-3'
Cyclin E1	NM_001238	Forward: 5'-GCAGTATCCCCAGCAAATC-3' Reverse: 5'-TCAAGGCAGTCAACATCCA-3'
Cyclin D1	NM_053056	Forward: 5'-GCTGTGCATCTACACCGACAACTC-3' Reverse: 5'-AGGTTCCACTTGAGCTTGTTCACC-3'
E2F3	NM_001949	Forward: 5'-CCAACTCAGGACATAGCGATTGCTC-3' Reverse: 5'-AGGAATTTGGTCCTCAGTCTGCTGT-3'
GAPDH	NM_002046	Forward: 5'-GCACCGTCAAGGCTGAGAAC-3' Reverse: 5'-TGGTGAAGACGCCAGTGGA-3'
p21	NM_000389	Forward: 5'-AGCAGAGGAAGACCATGTGGA-3' Reverse: 5'-GGAGTGGTAGAAATCTGTCATGCT-3'
p27	NM_004064	Forward: 5'-AGCTTGCCCGAGTTCTACTACAG-3' Reverse: 5'-ACCAAATGCGTGTCCTCAGAGT-3'
3'UTR cloning		
Cyclin E1	NM_001238	Forward: 5'-TTCTCGAGATCCTTCTCCACCAAAGACAGTT-3' Reverse: 5'-TTTCTAGAGAATGGATAGATATAGCAGCACTTACA-3'

The forward and reverse primers for 3'UTR cloning carried the *Xho*I and *Xba*I sites at their 5'-ends, respectively.

HSCs. Because miR-195 is categorized into the same family as miR-15b and miR-16 and has been reported to regulate cell cycle by targeting E2F3, CDK6, and cyclin D1 (Xu et al., 2009), we suspect the involvement of miR-195 in the proliferation of HSC and in type I IFN, in particular IFN-β, -induced inhibition of their growth.

Materials and Methods

Materials

Human HSC line LX-2 was donated by Dr. Scott L. Friedman (Mount Sinai School of Medicine, New York, NY) (Xu et al., 2005). Necessary reagents and materials were obtained from the

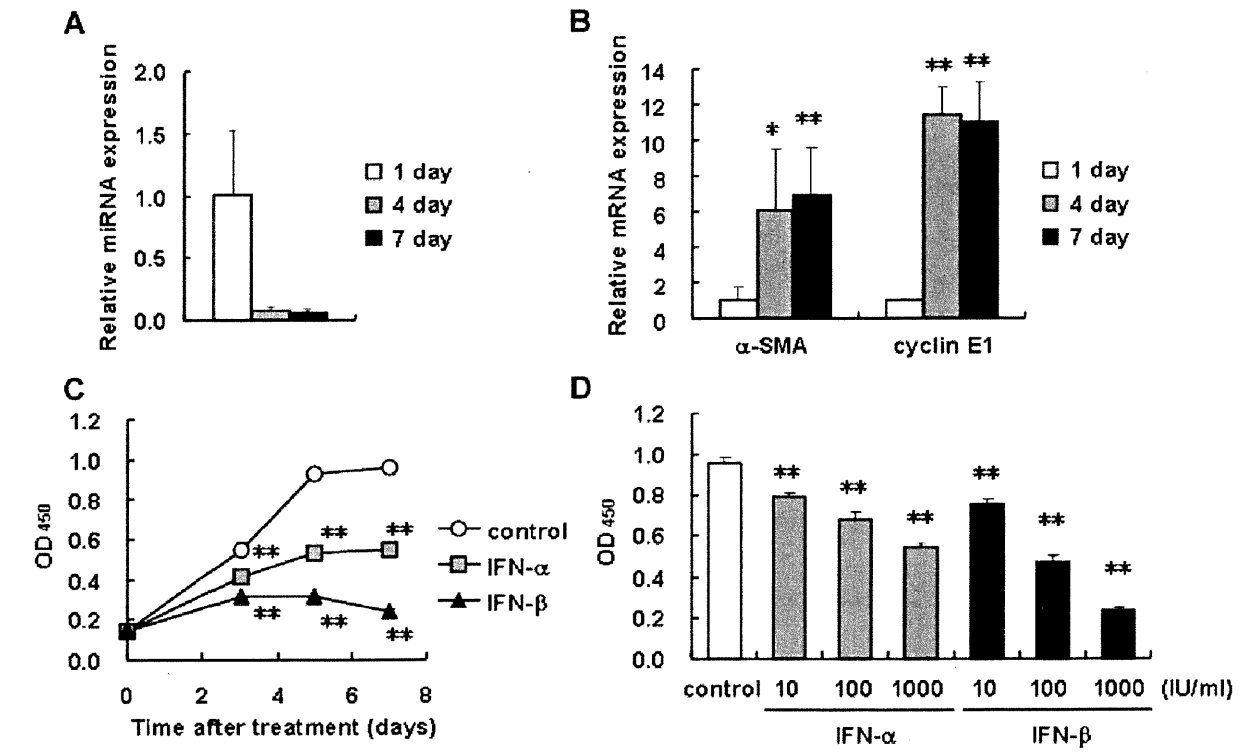

Fig. 1. Expression of miR-195 in mouse HSCs during primary culture and growth inhibitory effect of IFN-α and -β on human stellate cells. A,B: Isolated mouse HSCs were cultured for the indicated periods. The expression levels of miR-195 (A), and α-SMA and cyclin E1 mRNA (B) were measured by real-time PCR. *$P < 0.05$, **$P < 0.01$ compared with 1 day. C,D: LX-2 cells were incubated with IFN-α or -β (1,000 IU/ml) for 3–7 days (C), or with IFN-α or -β at the concentration of 10–1,000 IU/ml for 7 days (D). Control indicates non-treated cells. The proportion of viable cells was determined using a WST-1 assay. **$P < 0.01$ compared with control.

following sources: Dulbecco's modified Eagle's medium (DMEM) from Sigma Chemical Co. (St. Louis, MO); fetal bovine serum (FBS) from Invitrogen (Carlsbad, CA); human natural IFN-α and -β from Otsuka Pharmaceutical Co. (Tokushima, Japan) and Toray Industries, Inc. (Tokyo, Japan), respectively; precursor and inhibitor of miR-195, and the corresponding negative controls from Ambion (Austin, TX); mouse monoclonal antibody against cyclin E1, cyclin D1 and p21, and glyceraldehyde-3-phosphate dehydrogenase (GAPDH) from MBL (Nagoya, Japan), Cell Signaling Technology, Inc. (Beverly, MA), and Chemicon International, Inc. (Temecula, CA), respectively; rabbit polyclonal antibodies against cyclin-dependent kinase (CDK) 6 and E2F3 from Santa Cruz Biotechnology, Inc. (Santa Cruz, CA); goat polyclonal antibody against CDK4 from Santa Cruz Biotechnology, Inc.; enhanced Chemiluminescence plus detection reagent from GE Healthcare (Buckinghamshire, UK); Immobilon P membranes from Millipore Corp. (Bedford, MA); reagents for cDNA synthesis and real-time PCR from Toyobo (Osaka, Japan); a cell counting kit from Dojindo Laboratories (Kumamoto, Japan); and all other reagents from Sigma Chemical Co. or Wako Pure Chemical Co. (Osaka, Japan).

Cells

LX-2 cells were maintained in DMEM supplemented with 10% FBS (DMEM/FBS) and were plated at a density of 0.7–1.5 × 10^4 cells/cm^2 24 h prior to biological assay. Biological assays were done in DMEM/FBS unless stated otherwise. Mouse primary HSCs were isolated from male C57BL/6 mice by the pronase-collagenase digestion method as described previously (Uyama et al., 2006) and were cultured in DMEM/FBS.

Transient transfection of miRNA precursors and inhibitors

Precursor of miR-195, which was a double-strand RNA mimicking endogenous miR-195 precursor, and the negative control with a scrambled sequence were transfected into LX-2 cells using Lipofectamine 2000 (Invitrogen) at a final concentration of 50 nM in accordance with the manufacturer's instructions. Briefly, miRNA precursor and Lipofectamine 2000 were mixed at a ratio of 25 (pmol):1 (μl) in Opti-MEM I Reduced Medium (Invitrogen), incubated for 20 min at room temperature, and were then added to the cultures. After 24 h, the culture medium was replaced with fresh medium. Inhibitor of miR-195, which was designed to bind to endogenous miR-195 and inhibit its activity, and the negative control with a scrambled sequence were transfected similarly. After 6 h, the culture medium was changed and IFN-β was added successively.

Cell proliferation assay

LX-2 cells were plated at a density of 2 × 10^3 cells/well in 96-well plates 24 h prior to experiments. The culture medium was replaced by fresh medium containing different concentrations of IFNs at days 0 and 3. After 3, 5, and 7 days of treatment, cell proliferation was measured by WST-1 assay. In another experiment, the cells

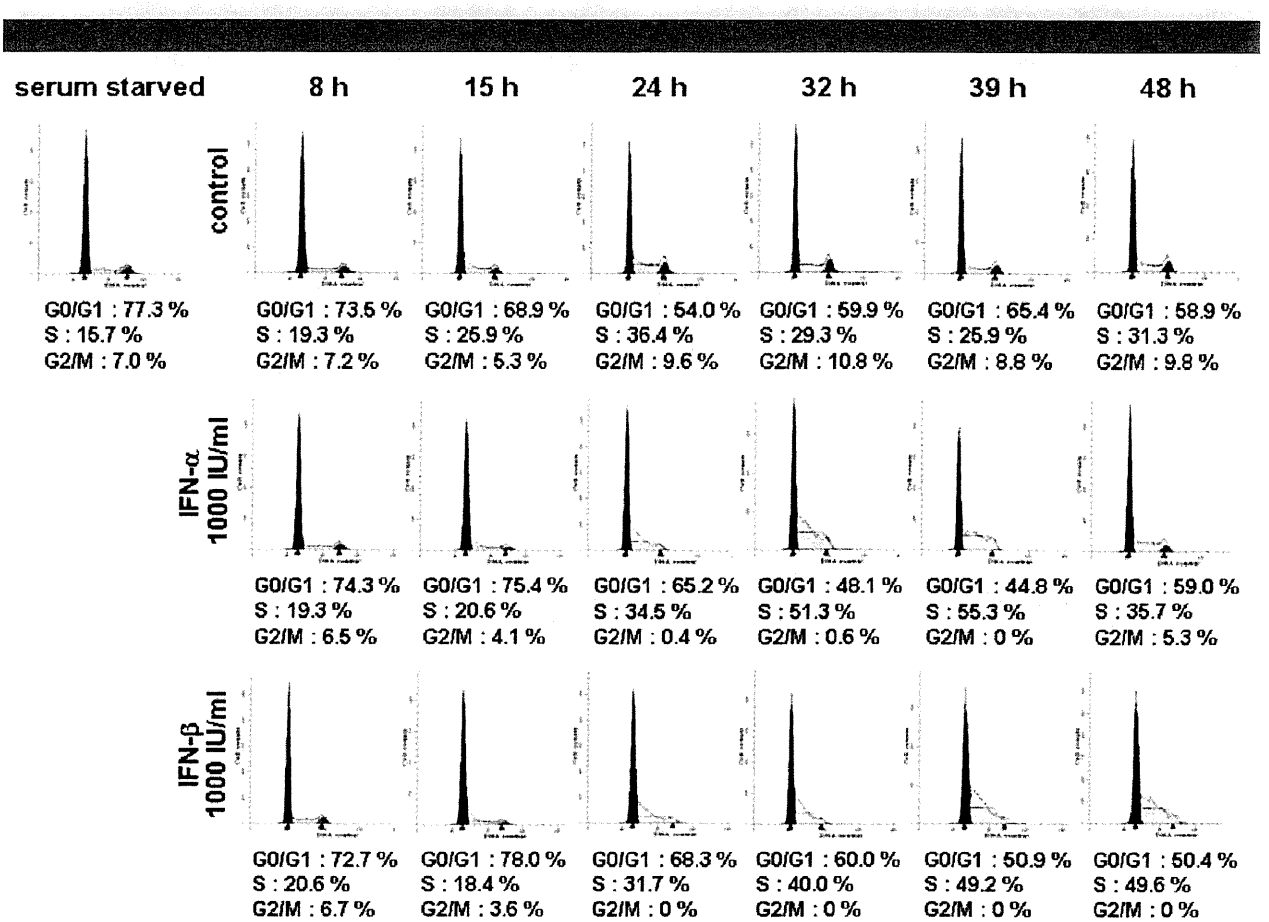

Fig. 2. Effect of IFN-α and -β on cell cycle distribution in human stellate cells. LX-2 cells synchronized in G0/G1 phase were then incubated with IFN-α or -β (1,000 IU/ml) in DMEM/FBS for the indicated periods. Control indicates non-treated cells. The cell cycle was analyzed by flow cytometry. The white, black, and shaded region indicates the histogram measured by flow cytometry, G0/G1 phase (left) or G2/M phase (right), and S phase, respectively, as analyzed by ModFIT LT software.

were plated at a density of 3×10^3 cells/well in 96-well plate for 24 h prior and were then transfected with the miR-195 precursor as described above. After 24 h, the medium was changed and the culture was continued for an additional 1–3 days before the measurement of cell proliferation.

Cell cycle analysis

Cells were serum starved for 24 h and then the medium was replaced with IFN-containing DMEM/FBS. At the indicated time points after treatment, the cells were harvested by trypsinization, washed in phosphate-buffered saline (PBS), and fixed in ice-cold 70% ethanol. The cells were washed in PBS and resuspended in PBS containing 500 μg/ml RNase A and incubated for 20 min. Cellular DNA was stained with propidium iodide at a final concentration of 25 μg/ml for 20 min. The cells were analyzed using a FACSCalibur HG flow cytometer (Becton Dickinson, Franklin Lakes, NJ). A total of 20,000 events were counted for each sample. Data were analyzed using ModFIT LT software (Verity Software House, Topsham, ME).

Quantitative real-time PCR

Quantitative real-time PCR was performed according to the method described elsewhere with use of a set of gene-specific oligonucleotide primers (Table 1) using an Applied Biosystems Prism 7500 (Applied Biosystems, Foster City, CA) (Ogawa et al., 2010). To detect miR-195 expression, the reverse transcription reaction was performed using a TaqMan microRNA Assay (Applied Biosystems) in accordance with the manufacturer's instructions. The expression level of GAPDH was used to normalize the relative abundance of mRNAs and miR-195.

Immunoblotting

Cells were lysed in RIPA buffer [50 mM Tris/HCl, pH 7.5, 150 mM NaCl, 1% NP-40, 0.5% sodium deoxycholate, 0.1% sodium dodecyl sulfate (SDS)] containing Protease Inhibitor Cocktail, Phosphatase Inhibitors Cocktail 1, and Phosphatase Inhibitor Cocktail 2 (Sigma). Proteins (20 μg) were electrophoresed in a 10% SDS–polyacrylamide gel and then transferred onto Immobilon P membranes (Ogawa et al., 2010). Immunoreactive bands were visualized by the enhanced chemiluminescence system using a Fujifilm Image Reader LAS-3000 (Fuji Medical Systems, Stamford, CT).

Luciferase reporter assay

Interaction of miR-195 to the 3′UTR of the cyclin E1 gene was tested according to the reported method (Ogawa et al., 2010). The 3′UTR of the cyclin E1 gene containing putative miR-195 target regions was obtained by PCR using cDNA derived from LX-2 and a primer set listed in Table 1. The obtained DNA fragments (497 bp) were inserted into a pmirGLO Vector (Promega, San Luis Obispo,

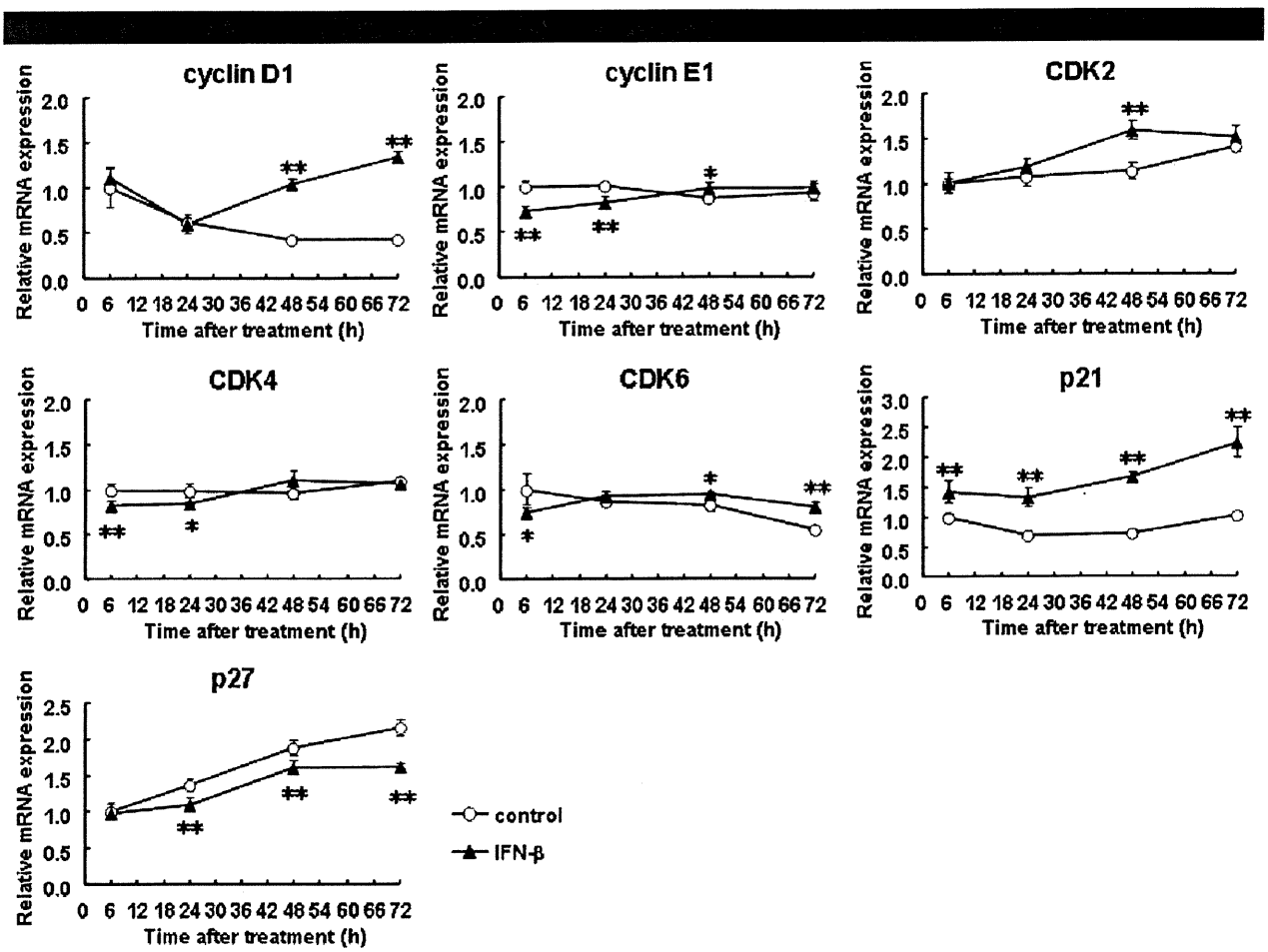

Fig. 3. Expression of cell cycle-related genes in stellate cells. LX-2 cells were incubated with IFN-β (1,000 IU/ml) for up to 72 h for determining the expression levels of mRNAs of cyclin D1, cyclin E1, CDK2, CDK4, CDK6, p21, and p27. Control indicates non-treated cells. *$P < 0.05$, **$P < 0.01$ compared with control.

CA). LX-2 cells, plated in 96-well plates at a density of 2×10^4 cells/well 24 h prior to experiment, were transfected with 200 ng of reporter plasmid and miRNA precursor using Lipofectamine 2000. After 24 h, the medium was changed to 20 μl of PBS. The Dual-Glo Luciferase Assay System (Promega) was used to analyze luciferase expression in accordance with the manufacturer's protocol. Firefly luciferase activity was normalized to *Renilla* luciferase activity to adjust for variations in transfection efficiency among experiments.

Statistical analysis

Data presented as graphs are the means ± SD of at least three independent experiments. Statistical analysis was performed using Student's *t*-test. $P < 0.05$ was considered significant.

Results

Reduction of miR-195 expression during activation of primary-cultured HSCs

It has been known that, when maintained in a plastic culture plate, freshly isolated primary-cultured HSCs undergo spontaneous activation and transformation into myofibroblastic cells that express α-SMA and produce fibrogenic mediators, such as type I collagen and transforming growth factor-β. In our preliminary experiments using primary-cultured mouse HSCs, we noticed that the cells drastically decreased the expression of miR-195 when they underwent spontaneous activation (unpublished observation). The present study confirmed this notion as shown in Figure 1A. miR-195 expression level certainly decreased in activation process of primary-cultured mouse HSCs. In contrast, the expression levels of α-SMA and cyclin E1 mRNA increased (Fig. 1B). Accordingly, we considered that miR-195 plays a role as an antiproliferative and antiactivating miRNA in HSCs. As a matter of fact, there was a study showing that miR-16 family including miR-195 inhibits proliferation of lung cancer cells by silencing cyclins D1 and E1, and CDK6 (Liu et al., 2008). The result indicated by Figure 1 and the cited study together drove us to explore the IFN's antiproliferative action on HSCs (Mallat et al., 1995; Shen et al., 2002), focusing on miR-195 and cell cycle-related genes.

Effects of IFN-α and -β on proliferation of HSCs

First, we investigated the effects of type I IFNs on the proliferation of LX-2 cells using a WST-1 assay. LX-2 cells in control culture continued to grow during the experimental

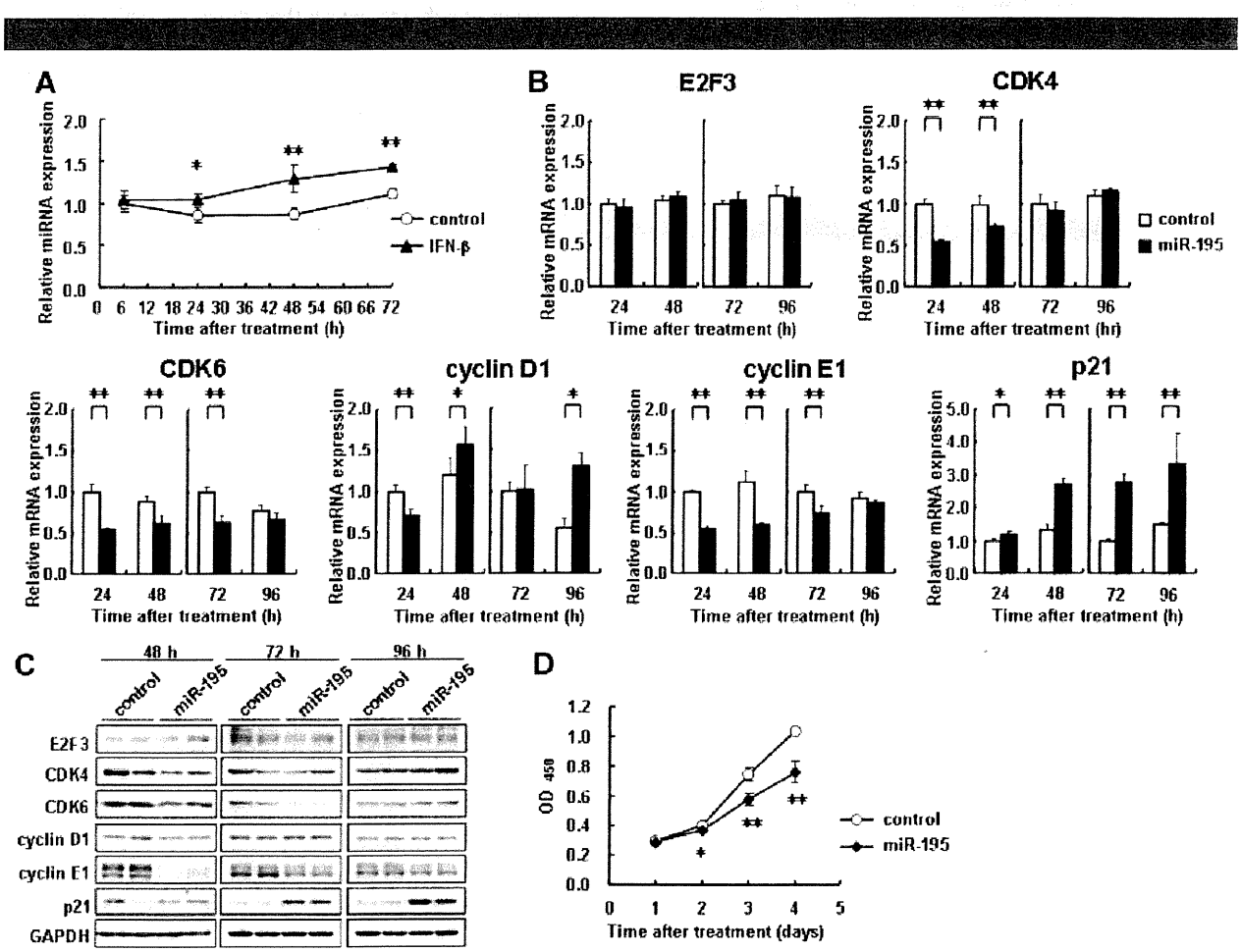

Fig. 4. Regulation of expression of cell cycle regulators by miR-195. A: LX-2 cells were incubated with IFN-β (1,000 IU/ml) for up to 72 h for determining the expression levels of miR-195. Control indicates non-treated cells. *$P < 0.05$, **$P < 0.01$ compared with control. B–D: LX-2 cells were transfected with 50 nM miR-195 precursor or a negative control (control). B: mRNA expression levels of E2F3, CDK4, CDK6, cyclin D1, cyclin E1, and p21 measured at 24, 48, 72, and 96 h post-transfection. C: Protein expression of E2F3, CDK4, CDK6, cyclin D1, cyclin E1, and p21 examined at 48, 72, and 96 h post-transfection. D: Growth of LX-2 cells transfected with 50 nM miR-195 precursor or a negative control (control) was measured using a WST-1 assay. *$P < 0.05$, **$P < 0.01$ compared with control.

period of 7 days (Fig. 1C). IFN-α and -β both, but the latter more actively, decreased cell proliferation time-dependently at a concentration of 1,000 IU/ml, supporting the previous studies (Mallat et al., 1995; Shen et al., 2002). Dose-dependency of the growth inhibition is shown in IFN concentrations from 10 to 1,000 IU/ml (Fig. 1D).

Effects of IFN-α and -β on cell cycle distribution

To elucidate the mechanism of the growth inhibitory effect of IFN, we next examined the change in cell cycle distribution in response to IFN-α and -β treatment by flow cytometry. LX-2 cells were synchronized in G0/G1 phase by serum starvation for 24 h. In non-treated cells (control), population in G0/G1 phase was reduced after serum exposure, which was accompanied by the increase of population in S phase. This cell cycle transition peaked at 24 h (Fig. 2, upper part). In cells treated with IFN-α or -β, the G0/G1 phase population was larger and the S phase population was smaller than in the control cells at 15 h and 24 h. In addition, the accumulation of cells in early S phase was observed at 32–48 h (Fig. 2, middle and lower parts). These delays in cell cycle shift were more potent in IFN-β-treated cells than in IFN-α-treated cells. It was concluded that type I IFN hampered HSC proliferation through a delay in the cell cycle at the transition from G1 to S phase and in the progression of S phase.

Regulation of cyclin E1 and p21 expression by IFN-β

IFN-β was chosen in the following experiments because of its more potent inhibition of cell cycle progression than IFN-α as described above. The transition from G1 to S phase and the progression of S phase are known to be influenced by various regulators (Golias et al., 2004). Among them, we found that IFN-β significantly decreased cyclin E1 mRNA expression levels by 0.6- to 0.7-fold at 6 and 24 h and increased p21 mRNA expression levels by 1.4- to 2.3-fold at 6, 24, 48, and 72 h in LX-2 cells (Fig. 3). The expression levels of CDK4 and CDK6 were also reduced by IFN-β at early phase with less extent. The others showed negligible change within 24 h although variable dynamics were seen thereafter; changes of cyclin D1, CDK2, and p27 expression at late phase were toward cell cycle promotion with currently unknown reason.

Regulation of miR-195 expression by IFN-β

The result indicated from Figure 1 strongly suggested the possibility that IFN-β increase the expression of miR-195 in LX-2 cells. To test this possibility, we examined the expression levels of miR-195 in IFN-β-treated LX-2 cells. As a result, the miR-195 expression level was significantly increased by IFN-β treatment at 24, 48, and 72 h (Fig. 4A).

Regulation of cyclin E1 and p21 expression by miR-195

The results obtained from experiments shown in Figures 3 and 4A led us to hypothesize that IFN-β up-regulates the expression of miR-195, which then down-regulates the expression of cyclin E1 and up-regulates the expression of p21. In addition, there had been a study reporting that miR-195 targets E2F3, CDK6, and cyclin D1 in addition to cyclin E1 (Xu et al., 2009). Under these considerations, we examined the changes in the expression levels of the above-mentioned cell cycle-related molecules and CDK4 by introducing miR-195

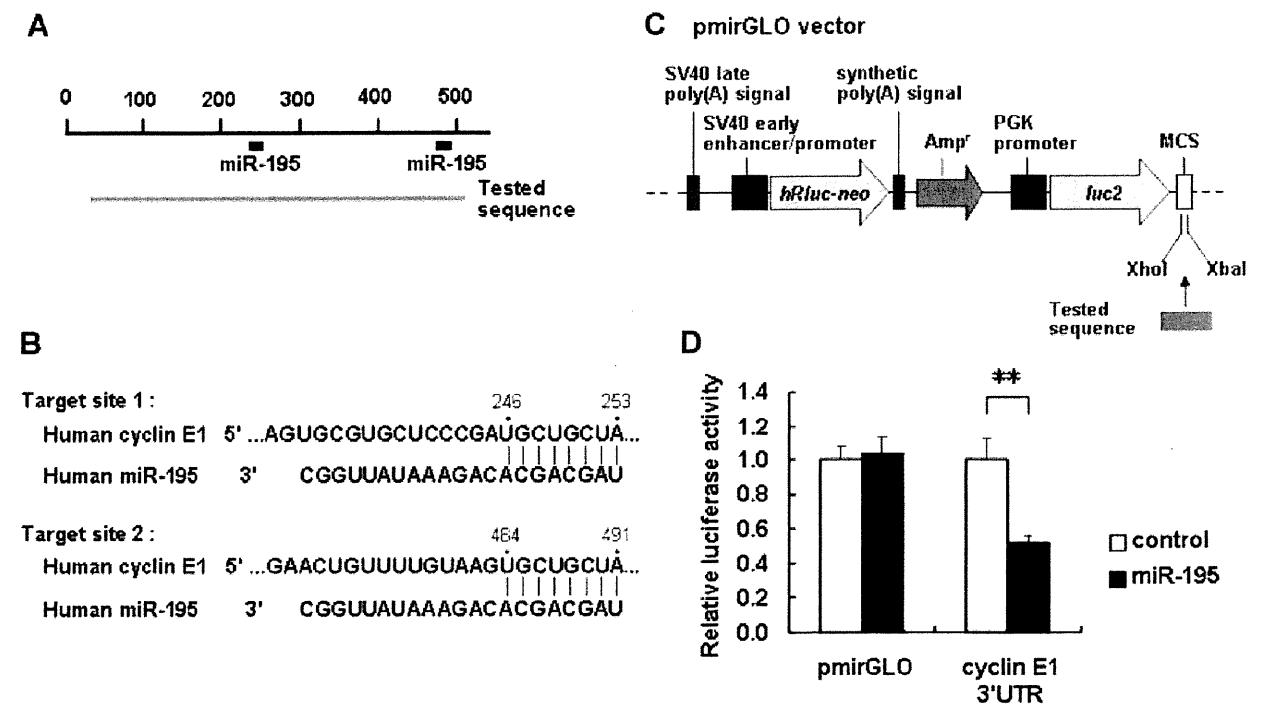

Fig. 5. Interaction of miR-195 with the 3′UTR of cyclin E1 mRNA. A: Schematic indication of the putative miR-195 target sites in the 3′UTR of the cyclin E1 mRNA. Tested sequences indicate the regions that were inserted into the luciferase reporter vector. B: Predicted pairing of the target region and miRNAs. C: Structure of the luciferase reporter vector (Ogawa et al., 2010). The putative miR-195 target region in cyclin E1 3′UTR (tested sequence) was ligated into the MCS. Arrows indicate the gene directions. Amp^R indicates an ampicillin resistance gene. D: Reporter gene assay of the interaction between the 3′UTR of cyclin E1 mRNA and miR-195 in LX-2 cells. Results are expressed as the relative activities against the activity in the presence of the control. $^*P < 0.05$, $^{**}P < 0.01$ compared with control.

precursor into LX-2 cells. Transfection of miR-195 precursor increased the miR-195 expression levels in LX-2 cells by up to 10,000–30,000 times compared with those in cells transfected with negative control (data not shown). Cyclin E1 mRNA and protein expression levels showed a remarkable reduction up to 72 h as result of miR-195 overexpression (Fig. 4B,C). On the other hand, p21 mRNA and protein expression levels showed a marked increase. CDK4, CDK6, and cyclin D1 expression levels were significantly changed at the mRNA level, but negligibly at the protein level. E2F3 mRNA and protein expression levels were unchanged (Fig. 4B,C). These results suggested that miR-195 mainly regulated cyclin E1 and p21 expression in LX-2 cells. Moreover, transfection of miR-195 precursor (50 nM) decreased the proliferation of LX-2 cells in the WST-1 assay (Fig. 4D). These results showed that miR-195 down-regulates endogenous cyclin E1 expression and up-regulates p21 expression, resulting in the attenuation of cell cycle progression and cell proliferation.

Interaction of miR-195 with cyclin E1 3′UTR in LX-2 cells

Next, we examined whether miR-195 interacted directly with cyclin E1 3′UTR in LX-2 cells. The predicted miRNA target sites for miR-195 in the cyclin E1 3′UTR were analyzed using TargetScan Human Release 5.1 (http://www.targetscan.org/). The cyclin E1 3′UTR contained two target sites for miR-195 (Fig. 5A,B). To investigate the direct interaction between them, the part of the cyclin E1 3′UTR containing the two miR-195 target sites (497 bp) was cloned from LX-2 cells, inserted the downstream of a firefly luciferase reporter gene in a pmirGLO vector (Fig. 5C), and cotransfected into LX-2 cells. As shown in Figure 5D, luciferase reporter activity decreased significantly in miR-195 precursor-transfected cells compared with cells transfected with a negative control of the precursor. These results suggested a direct interaction between miR-195 and cyclin E1 3′UTR in LX-2 cells. Binding site of miR-195 was not found in p21 3′UTR by TargetScan.

Regulation of cyclin E1 expression by IFN-β and miR-195

To confirm the contribution of miR-195 to the inhibitory effect of IFN-β on cyclin E1 expression, LX-2 cells were first transfected with 50 nM miR-195 inhibitor and then treated with 1,000 IU/ml IFN-β. As shown in Figure 6A, miR-195 inhibitor blocked the inhibitory effect of IFN-β on cyclin E1 mRNA expression at 16 and 24 h. Although there was no difference in the cyclin E1 mRNA expression between IFN-β-treated cells and non-treated cells (control) at 48 h, the cyclin E1 mRNA expression level in miR-195 inhibitor plus IFN-β-treated cells was up-regulated compared with non-treated cells (Fig. 6A). Immunoblot analysis revealed that miR-195 inhibitor elevated the cyclin E1 expression level of IFN-β-treated cells at 24 and 48 h (Fig. 6B).

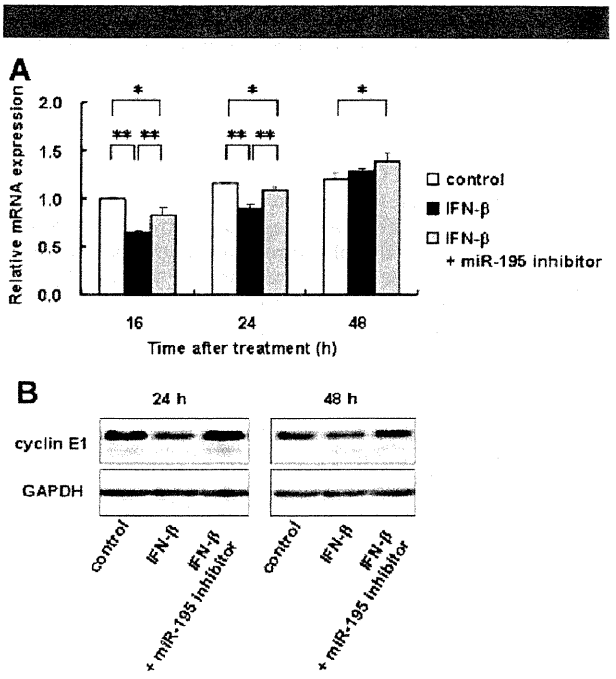

Fig. 6. Regulation of cyclin E1 expression by IFN-β and miR-195. LX-2 cells were transfected with 50 nM miR-195 inhibitor or a negative control. After 6 h, the culture medium was changed and then IFN-β (1,000 IU/ml) was added. Cells were then incubated for the indicated time periods. A: mRNA expression levels of cyclin E1. B: Protein expression levels of cyclin E1. GAPDH are for loading adjustment. Control; cells were transfected with a negative control and incubated without IFN-β. *$P<0.05$, **$P<0.01$.

Discussion

In this study, we showed that IFN-β is more antiproliferative on LX-2 cells than IFN-α, which appears to be contradictory to their known mechanism of action: both IFN-α and -β exert their activities through the common signaling pathway, beginning with binding to the same type I IFN receptor (IFNAR) consisting of IFNAR1 and IFNAR2, which activate the common components of janus kinase/signal transducer and activator of transcription (STAT) pathway (Darnell et al., 1994). However, a similar activity difference between the IFNs has also been demonstrated in colon cancer cell lines (Katayama et al., 2007) and in rat HSCs (Shen et al., 2002). Some studies showed that IFN-β but not IFN-α formed a stable complex with IFNARs, suggesting that IFN-β may interact with IFNAR chains in a manner different from IFN-α (Croze et al., 1996; Russell-Harde et al., 1999).

We showed here that IFN-β down-regulated the expression of cyclin E1 and up-regulated the expression of p21, which caused the cells to be less active proceeding in the transition from G0 to G1 phase and in the progression of S phase. The cell cycle is regulated by various molecules, such as cyclins and CDKs. Cyclin E is essential in activating CDK2. The cyclin E-CDK2 complex phosphorylates pRb at G1 phase, leading to gene transcription activities that are needed in S phase, and also activates the factors involved in DNA replication at early S phase (Golias et al., 2004). It has been reported that cyclin E1 expression increased in non-parenchymal cells of human fibrotic liver and that cyclin E1-deficient mice developed milder liver fibrosis compared with wild-type mice after CCl_4 administration (Nevzorova et al., 2010). These results imply that cyclin E1 regulates the progression of liver fibrosis by accelerating HSC proliferation.

The most frequent miRNAs that targets cyclin E1 are the miR-16 family, which consists of miR-15, -16, -195, -424, and -497 (Liu et al., 2008; Wang et al., 2009). We here observed the induction of miR-195 by IFN-β. miR-195 was reported to be down-regulated in human HCC tissues and to suppress HCC growth through the targeted interference of cyclin D1, CDK6, and E2F3 in a *xenograft* mouse model (Xu et al., 2009), while it was reported to target cyclin E1 in addition to the above-mentioned factors in A549 cells (Liu et al., 2008). miR-15b and miR-16 are down-regulated concomitantly with HSC activation and their overexpression induces apoptosis and a delay of cell cycle in HSCs by targeting Bcl-2 and cyclin D1 (Guo et al., 2009a,b). However, the role of miR-195 in HSCs remains unknown. We showed here that miR-195 expression was

decreased during spontaneous activation of primary-cultured mouse HSCs and that miR-195 interacted with cyclin E1 3′UTR and lowered the expression levels of the cyclin E1 mRNA and protein in LX-2 cells. These results suggest that the down-regulation of miR-195 may associate with the proliferation of HSCs in fibrotic liver similarly to miR-15 and miR-16. In this study, the changes of the protein expression levels of E2F3, CDK6, and cyclin D1, which were reported to be regulated by miR-195 (Xu et al., 2009), were negligible by miR-195, although the exact reason for this phenomenon was not determined. However, because the total context scores obtained by TargetScan were −0.73 for cyclin E1, −0.33 for E2F3, −0.32 for cyclin D1, and −0.09 for CDK6, the result obtained here was thought to be reasonable. In addition, minimal or negligible effect of miR-195 on the expression of E2F3, CDK4, CDK6, and cyclin D1 was compatible with that of IFN-β on these factors. Furthermore, inhibition of miR-195 by miR-195 inhibitor attenuated the effect of IFN-β on cyclin E1 expression, though not so strong. Taken together, it is most likely that the down-regulation of cyclin E1 by IFN-β treatment in HSCs is mediated through miR-195 up-regulation. The mechanism through which IFN-β induces miR-195 in LX-2 cells need to be explored further.

It is well known that IFNs induce the expression of p21 in various cancer cells (Sangfelt et al., 1999; Katayama et al., 2007). We also observed the up-regulation of p21 in IFN-β-treated cells. Therefore, p21, in addition to cyclin E1, may play a role in IFN-induced growth inhibition of HSCs. Until now, it has been reported that IFNs induce p21 expression through the binding of STAT and IFN regulatory factor, which are critical signaling molecules after IFN-IFNAR interaction, to p21 gene promoter (Gartel and Tyner, 1999). Unexpectedly, we found the up-regulation of p21 by miR-195 (Fig. 4). The results obtained here raise a new possibility that the up-regulation of p21 by IFN-β in HSCs may be partially mediated through miR-195.

In conclusion, type I IFN, in particular IFN-β, inhibited the proliferation of human HSCs by delaying the cell cycle in G1 to early S phase through the down-regulation of cyclin E1 and up-regulation of p21. The cyclin E1 down-regulation and p21 up-regulation were partially mediated by miR-195 that was up-regulated by IFN-β. This study raises a new mechanistic aspect of the antifibrotic effect of IFN in liver fibrosis and the possibility of influencing miR-195 as a therapeutic strategy for liver fibrosis.

Acknowledgments

This work was supported by a grant from the Ministry of Health, Labour and Welfare of Japan to N. Kawada (2008–2010).

Literature Cited

Bartel DP. 2004. MicroRNAs: Genomics, biogenesis, mechanism, and function. Cell 116:281–297.

Bataller R, Brenner DA. 2001. Hepatic stellate cells as a target for the treatment of liver fibrosis. Semin Liv Dis 21:437–451.

Chang XM, Chang Y, Jia A. 2005. Effects of interferon-alpha on expression of hepatic stellate cell and transforming growth factor-beta I and alpha-smooth muscle actin in rats with hepatic fibrosis. World J Gastroenterol 11:2634–2636.

Croze E, Russell-Harde D, Wagner TC, Pu H, Pfeffer LM, Perez HD. 1996. The human type I interferon receptor. Identification of the interferon beta-specific receptor-associated phosphoprotein. J Biol Chem 271:33165–33168.

Darnell JE, Kerr IM, Stark GR. 1994. Jak-STAT pathways and transcriptional activation in response to IFNs and other extracellular signaling proteins. Science 264:1415–1421.

Fort J, Pilette C, Veal N, Oberti F, Gallois Y, Douay O, Rosenbaum J, Cales P. 1998. Effects of long-term administration of interferon alpha in two models of liver fibrosis in rats. J Hepatol 29:263–270.

Friedman SL. 2000. Molecular regulation of hepatic fibrosis, an integrated cellular response to tissue injury. J Biol Chem 275:2247–2250.

Gartel AL, Tyner AL. 1999. Transcriptional regulation of the p21(WAF1/CIP1) gene. Exp Cell Res 246:280–289.

Golias CH, Charalabopoulos A, Charalabopoulos K. 2004. Cell proliferation and cell cycle control: A mini review. Int J Clin Pract 58:1134–1141.

Guo CJ, Pan Q, Jiang B, Chen GY, Li DG. 2009a. Effects of upregulated expression of microRNA-16 on biological properties of culture-activated hepatic stellate cells. Apoptosis 14:1331–1340.

Guo CJ, Pan Q, Li DG, Sun H, Liu BW. 2009b. miR-15b and miR-16 are implicated in activation of the rat hepatic stellate cell: An essential role for apoptosis. J Hepatol 50:766–778.

Inagaki Y, Nemoto T, Kushida M, Meng Y, Higashi K, Ikeda K, Kawada N, Shirasaki F, Takehara K, Sugiyama K, Fujii M, Yamauchi H, Nakao A, de Crombrugghe B, Watanabe T, Okazaki I. 2003. Interferon alpha down-regulates collagen gene transcription and suppresses experimental hepatic fibrosis in mice. Hepatology 38:890–899.

Ji JF, Shi J, Budhu A, Yu ZP, Forgues M, Roessler S, Ambs S, Chen YD, Meltzer PS, Croce CM, Qin LX, Man K, Lo CM, Lee J, Ng IOL, Fan J, Tang ZY, Sun HC, Wang XW. 2009a. MicroRNA expression, survival, and response to interferon in liver cancer. N Engl J Med 361:1437–1447.

Ji JL, Zhang JS, Huang GC, Qian J, Wang XQ, Mei S. 2009b. Over-expressed microRNA-27a and 27b influence fat accumulation and cell proliferation during rat hepatic stellate cell activation. FEBS Lett 583:759–766.

Katayama T, Nakanishi K, Nishihara H, Kamiyama N, Nakagawa T, Kamiyama T, Iseki K, Tanaka S, Todo S. 2007. Type I interferon prolongs cell cycle progression via p21(WAF1/CIP1) induction in human colon cancer cells. Int J Oncol 31:613–620.

Liu Q, Fu HJ, Sun F, Zhang HM, Tie Y, Zhu J, Xing RY, Sun ZX, Zheng XF. 2008. miR-16 family induces cell cycle arrest by regulating multiple cell cycle genes. Nucleic Acids Res 36:5391–5404.

Mallat A, Preaux AM, Blazejewski S, Rosenbaum J, Dhumeaux D, Mavier P. 1995. Interferon alpha and gamma inhibit proliferation and collagen synthesis of human Ito cells in culture. Hepatology 21:1003–1010.

Nevzorova YA, Bangen JM, Gassler N, Haas U, Weiskirchen R, Tacke F, Sicinski P, Trautwein C, Liedtke C. 2010. Cyclin E1 controls the cell cycle activity of hepatic stellate cells and triggers fibrogenesis in mice. J Hepatol 52:S374–S375.

Ogawa T, Kawada N, Ikeda K. 2009. Effect of natural interferon alpha on proliferation and apoptosis of hepatic stellate cells. Hepatol Int 3:497–503.

Ogawa T, Iizuka M, Sekiya Y, Yoshizato K, Ikeda K, Kawada N. 2010. Suppression of type I collagen production by microRNA-29b in cultured human stellate cells. Biochem Biophys Res Commun 391:316–321.

Pedersen IM, Cheng G, Wieland S, Volinia S, Croce CM, Chisari FV, David M. 2007. Interferon modulation of cellular microRNAs as an antiviral mechanism. Nature 449:919–922.

Pestka S, Langer JA, Zoon KC, Samuel CE. 1987. Interferons and their actions. Annu Rev Biochem 56:727–777.

Russell-Harde D, Wagner TC, Perez HD, Croze E. 1999. Formation of a uniquely stable type I interferon receptor complex by interferon beta is dependent upon particular interactions between interferon beta and its receptor and independent of tyrosine phosphorylation. Biochem Biophys Res Commun 255:539–544.

Sangfelt O, Erickson S, Castro J, Heiden T, Gustafsson A, Einhorn S, Grander D. 1999. Molecular mechanisms underlying interferon-alpha-induced G0/G1 arrest: CKI-mediated regulation of G1 Cdk-complexes and activation of pocket proteins. Oncogene 18:2798–2810.

Shen H, Zhang M, Minuk GY, Gong YW. 2002. Different effects of rat interferon alpha, beta and gamma on rat hepatic stellate cell proliferation and activation. BMC Cell Biol 3:9.

Tanabe J, Izawa A, Takemi N, Miyauchi Y, Torii Y, Tsuchiyama H, Suzuki T, Sone S, Ando K. 2007. Interferon-beta reduces the mouse liver fibrosis induced by repeated administration of concanavalin A via the direct and indirect effects. Immunology 122:562–570.

Uyama N, Zhao L, Van Rossen E, Hirako Y, Reynaert H, Adams DH, Xue Z, Li Z, Robson R, Pekny M, Geerts A. 2006. Hepatic stellate cells express synemin, a protein bridging intermediate filaments to focal adhesions. Gut 55:1276–1289.

Uze G, Schreiber G, Piehler J, Pellegrini S. 2007. The receptor of the type I interferon family. Curr Top Microbiol Immunol 316:71–95.

Venugopal SK, Jiang J, Kim TH, Li Y, Wang SS, Torok NJ, Wu J, Zern MA. 2010. Liver fibrosis causes downregulation of miRNA-150 and miRNA-194 in hepatic stellate cells, and their overexpression causes decreased stellate cell activation. Am J Physiol Gastrointest Liver Physiol 298:G101–G106.

Wang F, Fu XD, Zhou Y, Zhang Y. 2009. Down-regulation of the cyclin E1 oncogene expression by microRNA-16-1 induces cell cycle arrest in human cancer cells. BMB Rep 42:725–730.

Xu L, Hui AY, Albanis E, Arthur MJ, O'Byrne SM, Blaner WS, Mukherjee P, Friedman SL, Eng FJ. 2005. Human hepatic stellate cell lines, LX-1 and LX-2: New tools for analysis of hepatic fibrosis. Gut 54:142–151.

Xu T, Zhu Y, Xiong YJ, Ge YY, Yun JP, Zhuang SM. 2009. MicroRNA-195 suppresses tumorigenicity and regulates G(1)/S transition of human hepatocellular carcinoma cells. Hepatology 50:113–121.